Bulletin of Materials Science

Synthesis of standing ZnO nanosheets and impact of Ag nanoparticles loading on its optical property

--Manuscript Draft--

Manuscript Number:	BOMS-D-21-00755R1
Full Title:	Synthesis of standing ZnO nanosheets and impact of Ag nanoparticles loading on its optical property
Article Type:	Rapid Communication
Keywords:	Standing nanosheets; ZnO nanostructure; Ag nanoparticles; microwave-assisted hydrothermal
Corresponding Author:	Marjoni Imamora Ali Umar Institut Agama Islam Negeri Batusangkar Batusangkar, Padang, West Sumatera INDONESIA
Corresponding Author Secondary Information:	
Corresponding Author's Institution:	Institut Agama Islam Negeri Batusangkar
Corresponding Author's Secondary Institution:	
First Author:	Marjoni Imamora Ali Umar
First Author Secondary Information:	
Order of Authors:	Marjoni Imamora Ali Umar
	Setia Budi
	Muhammad Nurdin
	A. A. Umar
Order of Authors Secondary Information:	
Funding Information:	kementerian riset, teknologi dan pendidikan tinggi (FRGS/1/2019/STG02/UKM/02/3) — Assocc. Prof. Dr. A. A. Umar
Abstract:	Anisotropic nanostructures, such as nanosheets, nanorods, etc., in many cases, generate superior physicochemical properties over a highly symmetric structure counterpart. Here, we present a straightforward method to grow vertically oriented ZnO nanosheet directly on fluorine-tin oxide substrate using a microwave-assisted quasi-hydrothermal method. We also found that the Ag nanoparticles loading on the surface can effectively modify their optical properties, the potential for upgrading its performance in the existing applications. Due to the simplicity of the technique, Ag nanoparticles loaded standing ZnO nanosheet should find potential application in solar cells, sensing, and photocatalysis.
Response to Reviewers:	Dr. Amitava Patra Editor, Bulletin of Materials Science 12 August 2021 Dear Dr. Patra, We would like to say thank you very much for your email dated on July 31, 2021, regarding the revision our manuscript entitle “Synthesis of standing ZnO nanosheets and impact of Ag nanoparticles loading on its optical property” submitted to this journal with manuscript No. BOMS-D-21-00755. We also would like to say thank you to the reviewer for valuable suggestion and comment to this article. We then address carefully all the comments and suggestion by the reviewer and revise the manuscript accordingly. We use Track Change mode to show the revision that has been made in the articles. In the following, we summarize our responses to the

reviewer comments.

Reviewer #1: The authors report t a straightforward method to grow vertically oriented ZnO aniostropic nanosheet directly on FTO substrate using a microwave-assisted quasihydrothermal method. they have well characterized the films. It seems interesting and easy method although lots of reports are available on Ag/ZnO 1D nanostructure growth. It may further be considered if the following points are clarified:

Comment 1. What is PZN in Fig. 1?
Reply: We thank you very much to the reviewers for spotting this typos, PZN should read SZN for standing zinc oxide nanosheet. We have revised them accordingly in the entire manuscript.
Comment 2. How Al can be eliminated?
Reply: Actually, we have been attempting to remove the Al content in the sample and the process is still on going. We found that the Al existence in the sample is due to it is not fully consumed during the catalytic projection of ZnO nanosheet by the Al. We have control the Al layer thickness to obtain a suitable condition to produce ZnO nanosheet with free or minimum content of Al. To address this point, we add the following discussion in page 11.
“Nevertheless, the Al system is still detected in the sample with significant content as shown in XRD analysis result. This is the result of the Al layer is not fully consumed during the catalytic growth of SZN. It may certainly generate a strong effect to the optical and electrical properties of the SZN. At this stage, the approach to remove or to decrease the Al content in the SZN is not yet obtained. We assumed that the use of appropriate thickness of Al layer or the use of additonal catalytis to accelerate the Al consumption, might remove or reduce the Al presence in the SZN. This effort is being pursued and the result will be reported separately.”
Comment 3. FESEM images should be accompanied by the EDAX measurements. Without EDAX, how one verifies the elemental constituents of the films?
Reply: We agree with the reviewer that the EDAX can provide a detailed composition of the samples. Unfortunately, we have no access to the FESEM-EDAX since past several months so that we hope the present paper can be considered without EDAX analysis. It is because the presence of Ag, in particular, in the sample is verified by the optical absorbance spectra as shown in Figure 4, particularly Figure 4 and 4c. In the absorbance spectra (4a and 4c), we can see the existence of surface plasmon resonance absorption of Ag nanoparticles as 419 nm. This certainly is an indication of the Ag nanoparticles presence on the surface of the SZN.
We add the following paragraph in page 8 to address the point:
“The elemental analysis using electron energy dispersion spectroscopy (EDS) might further verify the Ag nanoparticles existence on the surface of SZN. Nevertheless, due to the limited access on the technique, we cannot provide them at this stage. However, the presence of such bright nanoparticles on the surface of SZN after a treatment in the Ag nanoparticles colloidal reaction is a clear indication that the Ag nanoparticles successfully decorate the SZN. Notwithstanding, the XRD and optical absorption analysis (will be discussed in the following) have confirmed that the Ag nanoparticles are axisting in SZN thin films.”
Comment 4. Ag loading is quite high as seen in FESEM. However, XRD shows an intensity of Ag even lower than Al peak.
Reply: We thank you the reviewer for highlighting this point that we overlooked to discuss earlier. We agree with the reviewer that the Ag nanoparticle loading is high as presented in FESEM analysis results. In XRD analysis, the Ag peaks is weaker than Al. This is due to the difference in the crystallite size where Al is higher than Ag nanoparticles. In growing the SZN, we deposited 30 nm thick Al layer on the entire substrate surface using thermal evaporation. This thickness could be too thick for projection of SZN during microwave assisted growth for 20 s. It is meant that not all the Al layer consumed during the catalytic growth of SZN. Because of Al layer exist on the entire substrate surface, its crystallite size could be higher than the Ag nanoparticles, which is only approximately 15 nm. Thus, the XRD peaks intensity of Al is higher than Ag nanoparticles.

We add a paragraph in page 8 to address this issue as follow:
“As the figure reveals, it is true that the peak intensity of the Ag nanoparticles is weak if compared even with the Al. Because the XRD peak intensity is related to the crystallite

size ratio of the component in the sample where SZN, particularly, majorly composes the sample, the diffraction peaks is dominated by the SZN leaving other crystallite component weakly observed in the XRD pattern. The Al peak intensity is higher than the Ag nanoparticles could be due to the same reason where Al layer crystallite size bigger than Ag nanoparticles. It is because Al layer does not completely consumed during the catalytic projection of SZN. The Al layer was deposited on the entire surface of the substrate with thickness of approximately 30 nm. An incomplete consumption of Al layer during the growth of SZN could leave the Al layer with crystallite size higher than Ag nanoparticles (size approximately 15 nm). Thus, the Al layer XRD peaks is higher than Ag nanoparticles."

Comment 5. How is the porosity of the films? Can it be estimated?

Reply: The porosity of the SZN films is quite difficult to be measured using standard tool such as Brunauer, Emmett and Teller (BET) analysis because this technique is mainly for powder specimen. In this work we estimated the porosity of the SZN based on the pore size (the average edge-to-edge distance) that was measured manually from the FESEM image. We found that the pore size decrease with the increasing of Zn+ precursors concentration. For example, at low precursor concentration, i.e. 0.01 M, the pore size is ca. 500 nm. Meanwhile, the pore size at the highest precursor concentration (0.05 M) is 50 nm. We have discussed this point in page 4.

Comment 6. Is it possible to grow in one pot like the report in CrystEngComm 15 (37), 7606 (2013)? If not, at least they should discuss the advantages of their work wrt to the reference.

Reply: At present stage, we did not evaluate the one-pot synthesis in preparing Ag nanoparticle modified SZN. While it is simple process, we thought that one-pot synthesis may deform the two-dimensional crystal growth of ZnO nanostructure due to the presence of Ag ion precursor in the reaction so that unique morphology properties will not be obtained. However, we address the issue in page 11 as follow:

"While the two-step method could be a tricky and lenghty process, not withstanding, it offers a sophisticated way to attain a preserved morphology of the SZN and the Ag nanoparticles. A simple, one-pot reaction process has been used to grow and modify the electrical and optical properties of the ZnO nanostructure as in the formation of Ag-ZnO nanorod[27]. Nevertheless, although it might produce effective modification on the optical properties of ZnO nanostructure, it may induce a deformation on the two-dimensional crystal growth in the ZnO. Therefore, special effort could be conducted to realize one-pot process for the preparation of Ag nanoparticles decorated SZN."

We also cite the reference suggested by the reviewer and label it as ref [27].

Comment 7. Why have not they taken glass substrate which is when seeded, ZnO 1D nanostructures can be grown easily.

Reply: Thank you for reviewer question on this point. We agree with the reviewer that the SZN could also be grown on the glass substrate as obtained in growing ZnO nanorods. We thought that the SZN should also be grown on glass substrate as well because of the unique catalytic effect of Al layer in promoting standing ZnO nanosheet. However, for the sake of FESEM analysis that requires a conducting substrate, we focused on growing the SZN on the FTO substrate.

We add the following sentences to address the reviewer question in page 11 as follow:

"We again remark that the Ag nanoparticles has effectively modified the optical properties of SZN, which was achieved via two-steps process. We predict that, although the present result use FTO as the substrate, the method should also be extended to grow SZN on other substrate, such as glass."

Finally, we hope the revised manuscript can now be accepted for publication in this journal. We very much appreciate your kind consideration and we are looking forwards to hearing from you at your earliest convenience.

Sincerely Yours,
Marjoni Imamora Ali Umar
Institut Agama Islam Negeri Batusangkar

Dr. Amitava Patra

Editor,

Bulletin of Materials Science

12 August 2021

Dear Dr. Patra,

We would like to say thank you very much for your email dated on July 31, 2021, regarding the revision our manuscript entitle "Synthesis of standing ZnO nanosheets and impact of Ag nanoparticles loading on its optical property" submitted to this journal with manuscript No. BOMS-D-21-00755. We also would like to say thank you to the reviewer for valuable suggestion and comment to this article.

We then address carefully all the comments and suggestion by the reviewer and revise the manuscript accordingly. We use Track Change mode to show the revision that has been made in the articles. In the following, we summarize our responses to the reviewer comments.

Reviewer #1: The authors report t a straightforward method to grow vertically oriented ZnO aniostropic nanosheet directly on FTO substrate using a microwave-assisted quasihydrothermal method. they have well characterized the films. It seems interesting and easy method although lots of reports are available on Ag/ZnO 1D nanostructure growth. It may further be considered if the following points are clarified:

Comment 1. What is PZN in Fig. 1?

Reply: We thank you very much to the reviewers for spotting this typos, PZN should read SZN for standing zinc oxide nanosheet. We have revised them accordingly in the entire manuscript.

Comment 2. How Al can be eliminated?

Reply: Actually, we have been attempting to remove the Al content in the sample and the process is still on going. We found that the Al existence in the sample is due to it is not fully consumed during the catalytic projection of ZnO nanosheet by the Al. We have control the Al layer thickness to obtain a suitable condition to produce ZnO nanosheet with free or minimum content of Al. To address this point, we add the following discussion in page 11.

"Nevertheless, the Al system is still detected in the sample with significant content as shown in XRD analysis result. This is the result of the Al layer is not fully consumed during the catalytic growth of SZN. It may certainly generate a strong effect to the optical and electrical properties of the SZN. At this stage, the approach to remove or to decrease the Al content in the SZN is not yet obtained. We assumed that the use of appropriate thickness of Al layer or the use of additonal catalytis to accelerate the Al consumption, might remove or reduce the

Al presence in the SZN. This effort is being pursued and the result will be reported separately."

Comment 3. FESEM images should be accompanied by the EDAX measurements. Without EDAX, how one verifies the elemental constituents of the films?

Reply: We agree with the reviewer that the EDAX can provide a detailed composition of the samples. Unfortunately, we have no access to the FESEM-EDAX since past several months so that we hope the present paper can be considered without EDAX analysis. It is because the presence of Ag, in particular, in the sample is verified by the optical absorbance spectra as shown in Figure 4, particularly Figure 4 and 4c. In the absorbance spectra (4a and 4c), we can see the existence of surface plasmon resonance absorption of Ag nanoparticles as 419 nm. This certainly is an indication of the Ag nanoparticles presence on the surface of the SZN.

We add the following paragraph in page 8 to address the point:

"The elemental analysis using electron energy dispersion spectroscopy (EDS) might further verify the Ag nanoparticles existence on the surface of SZN. Nevertheless, due to the limited access on the technique, we cannot provide them at this stage. However, the presence of such bright nanoparticles on the surface of SZN after a treatment in the Ag nanoparticles colloidal reaction is a clear indication that the Ag nanoparticles successfully decorate the SZN. Notwithstanding, the XRD and optical absorption analysis (will be discussed in the following) have confirmed that the Ag nanoparticles are axisting in SZN thin films."

Comment 4. Ag loading is quite high as seen in FESEM. However, XRD shows an intensity of Ag even lower than Al peak.

Reply: We thank you the reviewer for highlighting this point that we overlooked to discuss earlier. We agree with the reviewer that the Ag nanoparticle loading is high as presented in FESEM analysis results. In XRD analysis, the Ag peaks is weaker than Al. This is due to the difference in the crystallite size where Al is higher than Ag nanoparticles. In growing the SZN, we deposited 30 nm thick Al layer on the entire substrate surface using thermal evaporation. This thickness could be too thick for projection of SZN during microwave assisted growth for 20 s. It is meant that not all the Al layer consumed during the catalytic growth of SZN. Because of Al layer exist on the entire substrate surface, its crystallite size could be higher than the Ag nanoparticles, which is only approximately 15 nm. Thus, the XRD peaks intensity of Al is higher than Ag nanoparticles.

We add a paragraph in page 8 to address this issue as follow:

"As the figure reveals, it is true that the peak intensity of the Ag nanoparticles is weak if compared even with the Al. Because the XRD peak intensity is related to the crystallite size ratio of the component in the sample where SZN, particularly, majorly composes the sample, the diffraction peaks is dominated by the SZN leaving other crystallite component weakly observed in the XRD pattern. The Al peak intensity is higher than the Ag nanoparticles could be due to the same reason where Al layer crystallite size bigger than Ag nanoparticles. It is because Al layer does not completely consumed during the catalytic projection of SZN. The Al layer was deposited on the entire surface of the substrate with thickness of approximately 30 nm. An incomplete consumption of Al layer during the growth of SZN could leave the Al

layer with crystallite size higher than Ag nanoparticles (size approximately 15 nm). Thus, the Al layer XRD peaks is higher than Ag nanoparticles."

Comment 5. How is the porosity of the films? Can it be estimated?

Reply: The porosity of the SZN films is quite difficult to be measured using standard tool such as Brunauer, Emmett and Teller (BET) analysis because this technique is mainly for powder specimen. In this work we estimated the porosity of the SZN based on the pore size (the average edge-to-edge distance) that was measured manually from the FESEM image. We found that the pore size decrease with the increasing of Zn+ precursors concentration. For example, at low precursor concentration, i.e. 0.01 M, the pore size is ca. 500 nm. Meanwhile, the pore size at the highest precursor concentration (0.05 M) is 50 nm. We have discussed this point in page 4.

Comment 6. Is it possible to grow in one pot like the report in CrystEngComm 15 (37), 7606 (2013)? If not, at least they should discuss the advantages of their work wrt to the reference.

Reply: At present stage, we did not evaluate the one-pot synthesis in preparing Ag nanoparticle modified SZN. While it is simple process, we thought that one-pot synthesis may deform the two-dimensional crystal growth of ZnO nanostructure due to the presence of Ag ion precursor in the reaction so that unique morphology properties will not be obtained. However, we address the issue in page 11 as follow:

"While the two-step method could be a tricky and lenghty process, not withstanding, it offers a sophisticated way to attain a preserved morphology of the SZN and the Ag nanoparticles. A simple, one-pot reaction process has been used to grow and modify the electrical and optical properties of the ZnO nanostructure as in the formation of Ag-ZnO nanorod[27]. Nevertheless, although it might produce effective modification on the optical properties of ZnO nanostructure, it may induce a deformation on the two-dimensional crystal growth in the ZnO. Therefore, special effort could be conducted to realize one-pot process for the preparation of Ag nanoparticles decorated SZN."

We also cite the reference suggested by the reviewer and label it as ref [27].

Comment 7. Why have not they taken glass substrate which is when seeded, ZnO 1D nanostructures can be grown easily.

Reply: Thank you for reviewer question on this point. We agree with the reviewer that the SZN could also be grown on the glass substrate as obtained in growing ZnO nanorods. We thought that the SZN should also be grown on glass substrate as well because of the unique catalytic effect of Al layer in promoting standing ZnO nanosheet. However, for the sake of FESEM analysis that requires a conducting substrate, we focused on growing the SZN on the FTO substrate.

We add the following sentences to address the reviewer question in page 11 as follow:

"We again remark that the Ag nanoparticles has effectively modified the optical properties of SZN, which was achieved via two-steps process. We predict that, although the present result use FTO as the substrate, the method should also be extended to grow SZN on other substrate, such as glass."

Finally, we hope the revised manuscript can now be accepted for publication in this journal. We very much appreciate your kind consideration and we are looking forwards to hearing from you at your earliest convenience.

Sincerely Yours,

Marjoni Imamora Ali Umar
Institut Agam Islam Negeri Batusangkar

Synthesis of standing ZnO nanosheets and impact of Ag nanoparticles loading on its optical property

Marjoni Imamora Ali Umar*[1] , Setia Budi[2] , Muhammad Nurdin[3], and Akrajas Ali Umar*[4]

[1]Department of Physical Education, Faculty of Tarbiyah, Insitut Agama Islam Negeri Batusangkar, Batu Sangkar, 27213 West Sumatera, Indonesia.

2Department of Chemistry, Faculty of Mathematics and Natural Science, Universitas Negeri Jakarta, 13220 DKI Jakarta, Indonesia.

[3]Department of Chemistry, Faculty of Mathematics and Natural Science, Universitas Halu Oleo, Kendari, 93232 South-East Sulawesi, Indonesia.

[4]Institute of Microengeineering and Nanoelectronics, Universiti Kebangsaan Malaysia, 43600 UKM Bangi, Selangor, Malaysia.

*Corresponding Author: marjoniimamora@gmail.com (MIAU), akrajas@ukm.edu.my (AAU).

Abstract

Anisotropic nanostructures, such as nanosheets, nanorods, etc., in many cases, generate superior physicochemical properties over a highly symmetric structure counterpart. Here, we present a straightforward method to grow vertically oriented ZnO nanosheet directly on fluorine-tin oxide substrate using a microwave-assisted quasi-hydrothermal method. We also found that the Ag nanoparticles loading on the surface can effectively modify their optical properties, the potential for upgrading its performance in the existing applications. Due to the simplicity of the technique, Ag nanoparticles loaded standing ZnO nanosheet should find potential application in solar cells, sensing, and photocatalysis.

Keywords: Standing nanosheets; ZnO nanostructure; Ag nanoparticles; microwave-assisted hydrothermal.

1. Introduction

The morphology of the nanocrystals gives a strong influence on the overall properties of the materials[1-3]. This is the result of the modification of the confinement potential of the charge carrier when the shape of the nanocrystals is distorted under the quantum regime[4]. For example for the case of Au or Ag nanoparticles, their surface plasmonic resonance changes from single localized surface resonance to two localized surface plasmon resonance characters when their morphology transformed from spherical nanoparticles to nanorods or nanoplates morphology[5-8]. A similar case is also encountered in the ZnO nanocrystals[9, 10]. For example, its excitonic photoluminescence properties redshifted from 369 nm to 371 nm when its morphology altered from spherical to nanorods, respectively[11]. Not only excitonic-related photoluminescence shift but also the nature of defect-related photoluminescence, i.e. blueshifted from 528 nm to 514 nm when the nanostructure shape changes from spherical to nanorods, respectively. In addition, owing to the alteration of the surface atom when the morphology of the nanostructure changes, their surface physicochemical properties are strongly transformed. This results in the enhancement of the surface reactivity in sensing[12], photocatalysis[13, 14], surface biological activity[15, 16], and solar cells[17] when the morphology of ZnO nanostructure is modified from highly symmetrical spherical morphology to anisotropic shapes, such as nanorods, nanoplates, etc[18]. Considering the nature of physicochemistry transformation under morphology shift, the attempt to continuously prepare ZnO nanostructure with exotic anisotropic morphology should be demonstrated.

In this study, a simple and rapid method to grow a standing nanosheet of ZnO directly on the substrate surface is demonstrated via a microwave-assisted quasi-hydrothermal method[19]. In the typical process, the standing nanosheet has a length up to 1 μm and the thickness of the nanosheet is approximately 10 nm. The nanosheet growth direction on the surface is random, producing a pore-like surface, the result of the nanosheet network on the surface. We also found that the optical property of the standing ZnO nanosheet significantly modified upon being decorated with Ag nanoparticles of size from 15 to 20 nm on their surface, which is hardly achieved in other systems such as nanorods or other morphologies. An optical energy gap red-shifting up to 0.04 eV was observed, signifying its potential for

improved photo-activity properties in the application. The Ag nanoparticles loaded standing nanosheet of ZnO may find use in solar cells and non-linear optics applications.

2. Experimental

2.1. Ag nanoparticles (AgNPs)-loaded standing ZnO nanosheet (Ag-SZN) preparation.

AgNPs-loaded standing ZnO nanosheet (Ag-SZN) on a fluorine-doped Indium Tin oxide (FTO) substrate were prepared by a two-step process, i.e. SZN growth and AgNPs loading onto the SZN structure. The SZN on FTO substrate (Sigma Aldrich, the sheet resistance of ca. 10 Ω/square) was prepared by using our previously reported technique, namely microwave-assisted hydrolysis seed-mediated growth process[19]. Briefly, a cleaned FTO substrate that has been undergone a standard cleaning process in acetone and ethanol under an ultrasonication was sputtered with a thin layer of Al film (thickness approximately 30 nm) using an RF Magnetron Sputter machine. After following a further brief-cleaning process under ultrasonication in ethanol, ZnO nanoseeed of size approximately from 3 to 10 nm were deposited on the Al layer using alcohothermal seeding method[20], namely consecutive spin-coating of ethanolic solution of zinc nitrate hydrate, $ZnNO_3.6H_2O$ (Alfa Aesar) and thermal annealing (using a split-tube furnace system (Thermcraft, USA)) at 200 °C in air for 1 h. The SZN was then grown by simply immersing the FTO/Al loaded ZnO nanoseed substrate into a growth solution that contains an equimolar (0.3 M) aqueous solution of $ZnNO_3.6H_2O$ and 0.03 M hexamethytetramine (HMT). The growth reaction was carried out under microwave irradiation (power ca.~ 1100 W) inside a microwave oven (Panasonic) for 20 s. The sample was then taken out, washed in a copious amount of pure water, and dried using a flow of nitrogen gas. The ~~as~~ as-prepared SZNs were then annealed for 1 h in the air at 350 °C to remove any organic residue on the sample and to obtain a better ZnO crystallinity. From this procedure, a high-density SZN structure on the FTO substrate (confirmed by XRD and FESEM results) will be obtained. In this study, the SZN with five different porous densities were prepared by simply varying the Zn precursor ($ZnNO_3.6H_2O$) concentrations in the reaction, namely 0.01, 0.02, 0.03, 0.04, and 0.05 M. Other reagents and procedures used in this work were kept unchanged.

The Ag nanoparticle (AgNPs)-loaded SZN (Ag-SZN) were prepared by firstly immersing the SZN-coated FTO substrate into a 20 mL aqueous solution that contains 0.5 ml of 0.01 M $AgNO_3$ (Sigma-Aldrich, USA) and 0.5 ml of 0.01 M trisodium citrate (WAKO Chemical, Japan). The sample was left for 30 min undisturbed to facilitate Ag+ ions

adsorption onto the SZN surface. After that, 0.1 mL of ice-cooled $NaBH_4$ (0.1 M) was injected into the solution. The color of the solution changed from colorless to yellow, indicating the formation of Ag both in the solution and on the surface of SZN. The reaction was then left undisturbed for another 1.5 h at room temperature, to facilitate the effective growth of Ag nanoparticles on the surface of SZN. The sample was then taken out, washed with a copious amount of pure water, and finally dried with a flow of nitrogen gas. Finally, the sample was annealed in air at 200 °C for 1 h to remove any organic residue on the sample surface.

2.2. Characterizations

The morphologies of the unloaded and Ag-SZN were obtained using a field emission scanning electron microscopy (FESEM) Zeiss Supra 55VP FESEM apparatus. The phase and structural properties of the unloaded and Ag-SZN were characterized by X-ray diffraction (XRD) measurements using Bruker D8Advance with CuKα radiation (λ=1.541Å) and scan rate as low as 2°/min. UV-Vis diffuse reflectance spectroscopy (Winlab, Hitachi, Japan) was used to obtain the optical properties of the sample.

3. Results and Discussion

3.1 Ag nanoparticle-loaded SZN

Standing ZnO nanosheet (SZN) with controlled porous density on the FTO substrate surface has been successfully prepared using the present method. Figure 1 shows the typical surface morphology of the SZN grown using five different Zn precursor concentrations, namely 0.01, 0.02, 0.03, 0.04, and 0.05 M. As Figure 1 reveals, the SZNis characterized by a continuously connected nanosheet structure that is vertically grown on the substrate surface, forming a porous surface structure. The thickness of the nanosheet is in the range of 10 to 15 nm and was found to have no significant dependency on the Zn precursors concentration used in the reaction. However, the pore size (the average edge-to-edge distance) decreases with the increase of ZnO precursor concentration in the reaction. For example, at low concentration (see Figure 1a), the size of the pore is approximately 500 nm. The pore size effectively decreases when the precursor concentration was increased (Figure 1a-e). At a relatively high concentration, i.e. 0.05 M (see Figure 1 e), the pore size is as low as ca. 50 nm. This produces

SZN with high-pore density on the substrate surface, promising unique optical and electrical properties. A complete porosity data of nanosheet film grown from different ZnO precursor concentrations is summarized in Table 1. The increasing of the pore density upon the increasing of ZnO precursor concentration is simply related to the high-kinetic nature of the growth reaction at high precursor concentration causing rapid growth and deposition of the ZnO nanostructure onto the surface[21, 22]. Therefore, at this condition, the competitive nucleation characteristic of the reaction is high, resulting in the formation of smaller pore size, thus increases the density. Unfortunately, as can be seen from the figure, the use of high ZnO precursor concentration has caused un-stability in the reaction that was indicated by an active formation of ZnO by-product in solution (ZnO nanorods), of which some of them are attached to the nanosheet surface. This could more or less distort the unique property of the porous nanosheet film. The results are shown in Figures 1e and 1f (it's a magnified image).

The formation of nanosheet structure has been understood as the effect of effective etching and passivation of (101) and (100) planes by the $Al(OH)_4^-$ complexes in the solution that is produced from the dissolution of the Al layer by hexamethylene tetramine[19]. This condition favors the growth of two-dimensional morphology instead of other morphologies, such as spherical or irregular shape nanostructures.

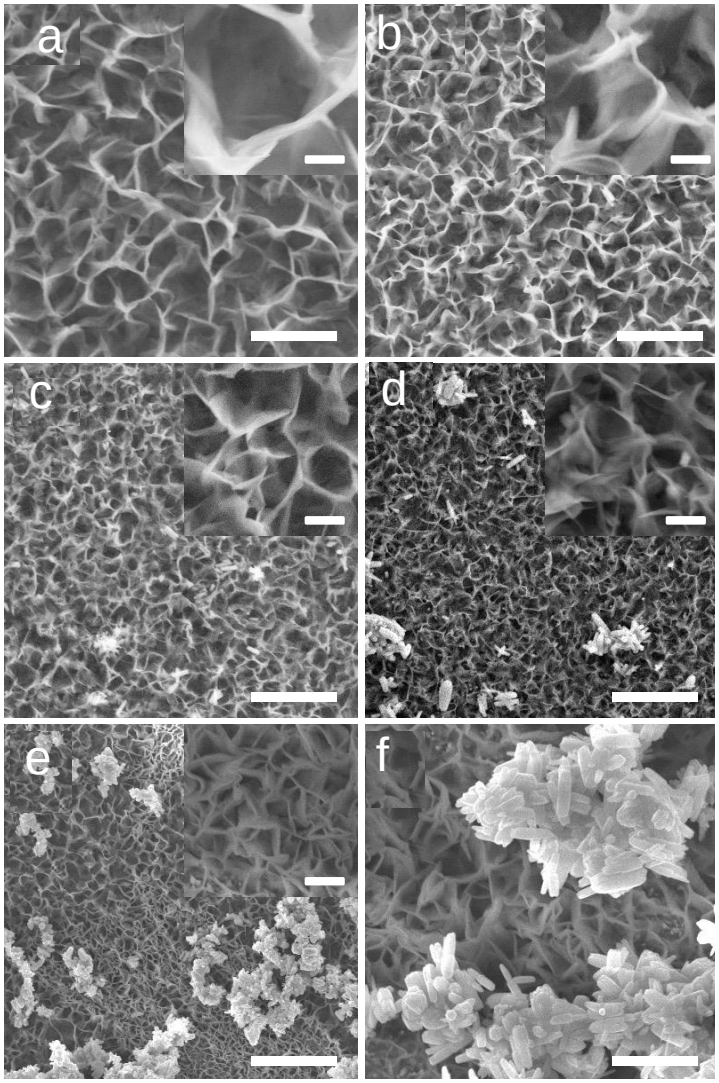

Figure 1. FESEM micrograph for ~~PZNs~~ SZNs morphology at various Zn+ precursor molarities, namely (a) 0.01, (b) 0.02, (c) 0.03, (d) 0.04, and (e) 0.05 M. (f) shows a high magnification image for sample E. Scale bars are 1 μm and 100 nm for insets and f.

Figure 2 shows the phase analysis result of the SZN that were prepared using five different Zn+ precursor solutions, namely 0.01, 0.02, 0.03, 0.04, and 0.05 M. As can be seen from the figure, the entire sample shows a similar XRD pattern with the presence of five major peaks in the spectrum, namely at 2θ of 31.6, 34.3, 36.2, 47.5 and 56.6°. This XRD pattern agrees well with the standard XRD diffraction data (file no. 36-1451) for the pure ZnO phase with peaks at 2θ of 31.6, 34.3, 36.2, 47.5, and 56.6° corresponding to the XRD diffraction from the (100), (002), (101) (102), and (111) Bragg planes, respectively. It can be

noted here that the SZN produce from the lower precursor concentration seems to be characterized by the (002) plane (*c*-axis plane) because of a high-diffraction intensity originated from this plane (see curve a). However, the XRD profile was effectively modified when the SZN was prepared using a higher ZnO precursor concentration (see curves b to e). At these concentrations, the SZN were characterized by (101) plane with ratio diffraction intensity between (101) and (002) planes as high as 1.5, which is only 0.5 for sample a. It is also observed that the diffraction from the (100) plane is also high and comparable to the (002) plane with an intensity ratio between (100) and (002) in the range of 0.6 to 0.8, which is only 0.4 for the sample a. We assumed that the SZN wall should be characterized by the plane of (101) and (100) planes. As the (101) and (100) planes for ZnO is a highly energetic surface, thus we expect peculiar optical and electrical properties can be produced from this structure. In addition, from the spectra, the Al crystal peaks were also present, namely at 38.0 and 56.5°. This could be from the Al layer that is not completely consumed during the SZN formation. However, their intensity is relatively low and its effect on the optical and electrical properties of SZN ~~are~~ is expected to be minimum.

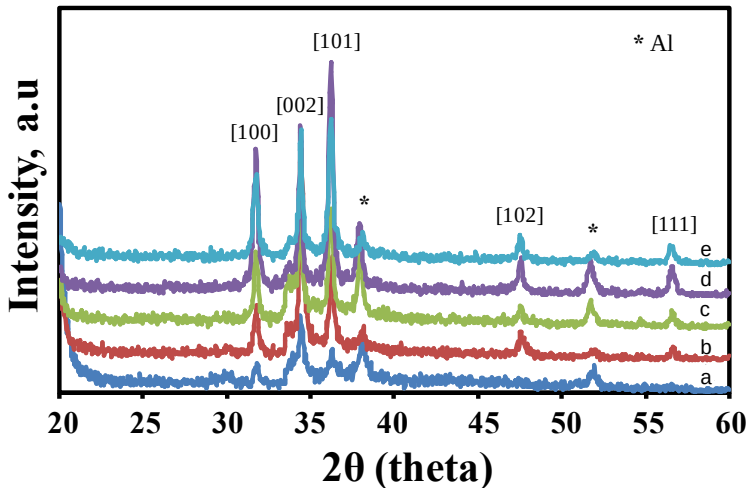

Figure 2. XRD spectra for ~~PZNs~~ SZNs morphology at various Zn+ precursor molarities of (a) 0.01, (b) 0.02 and (c) 0.03 (d) 0.04 and (e) 0.05 M shown respectively.

We then grew Ag nanoparticles onto the surface of SZN by our previously reported technique that involves a simple immersion of the SZN sample into the solution of Ag colloidal reaction formation. After finishing the Ag nanoparticle growth procedure for 1.5 h and followed by brief rinsing using pure water, we carried out a FESEM analysis to confirm the Ag nanoparticles formation on the SZN surface. The result is shown in Figure 3. As

Figure 3 shows, the Ag nanoparticles have been effectively attached to the surface of the SZN. They are indicated as bright dotted particles as shown in the high-resolution FESEM image in the inset of the corresponding FESEM image (see Figure 3a-e). Their size range from 15 to 20 nm. The elemental analysis using electron energy dispersion spectroscopy (EDS) might further verify the Ag nanoparticles existence on the surface of SZN. Nevertheless, due to the limited access to the technique, we cannot provide them at this stage. However, the presence of such bright nanoparticles on the surface of SZN after a treatment in the Ag nanoparticles colloidal reaction is a clear indication that the Ag nanoparticles successfully decorate the SZN. Notwithstanding, the XRD and optical absorption analysis (will be discussed in the following) has confirmed that the Ag nanoparticles are existing in SZN thin films.

We then performed an XRD analysis of the sample to further verify the existence of the Ag nanoparticles in the sample. A sample with medium Zn precursor concentration, i.e. 0.03 M, was used in the analysis. As has been expected, the Ag crystalline phase is observed in the XRD spectrum along with the ZnO and Al (see Figure 3f). The SZN decorated with Ag nanoparticles should produce special properties so that unusually high performance in the application would be obtained. As the figure reveals, the peak intensity of the Ag nanoparticles is indeed weak if compared even with the Al. Because the XRD peak intensity is related to the crystallite size ratio of the component in the sample where SZN, particularly, majorly composes the sample, the diffraction peaks are dominated by the SZN leaving other crystallite components weakly observed in the XRD pattern. The Al peak intensity is higher than the Ag nanoparticles could be due to the same reason where Al layer crystallite size is bigger than Ag nanoparticles. It is because Al layer is not completely consumed during the catalytic projection of SZN. The Al layer was deposited on the entire surface of the substrate with a thickness of approximately 30 nm. An incomplete consumption of Al layer during the growth of SZN could leave the Al layer with crystallite size higher than Ag nanoparticles (size approximately 15 nm). Thus, the Al layer XRD peak is higher than Ag nanoparticles.

We ~~then~~ carried out a UV-Vis absorption spectroscopy technique to further verify the presence of Ag nanoparticles on the surface of SZN and to evaluate~~d~~ the optical properties of the SZN under the influence of Ag nanoparticles attachment. Figure 4a shows their corresponding optical absorbance. It is seen that excitonic absorption of ZnO (at the wavelength of ca. 360 nm) [23] along with localized surface plasmon resonance absorption of Ag (ca. 419 nm) [24] are observed in the spectrum. This certainly is a further confirmation of the Ag nanoparticle's existence on the surface of SZN. As can be seen from Figure 4b and

Table 1, it can be estimated that there is a modification in the optical bandgap of the SZN when its dimension is altered due to the dimensional effect at this nanostructure regime or decorated with the Ag nanoparticle. We then extrapolate the Tauc plot from the absorbance spectrum of the sample to see the impact of dimension modification and the Ag nanoparticle attachment on the optical properties of the SZN (see Figure 4b). For example, the thinnest SZN (curve 1 in Figure 4b) decorated with the Ag nanoparticles has an optical band edge as high as 3.31 eV. It gradually decreases with the increase of thickness and has an optical energy gap as low as 3.29 eV in the thick~~n~~es~~ts~~ ZnO nanosheet (curve 5 in Figure 4b). Because the Ag nanoparticles dimension and density on the SZN surface are more or less similar on each SZN sample, as expected, we can remark that the energy gap decrease should be due to the increasing of SZN dimension and thicknes[25]. To understand the extent effect of Ag nanoparticle impact on the optical properties of the standing ZnO nanosheet, we compared the optical properties of pristine standing ZnO nanosheet with the ones decorated with Ag nanoparticles that were prepared using similar ZnO precursor concentration (0.04 M). The result is shown in Figures 4c and d. We noticed that the band edge of the ZnO is blue-shifted up to 0.04 eV with the attachment of Ag nanoparticles (Figure 4d). The pristine SZN optical band edge is approximately 3.25 eV. This result is quite surprising as surface attachment of the Ag nanoparticles in fact can induce the bulk optical properties of the SZN, which could be via many ways such as carrier equilibration effect, Fermi level alignment between the Ag and ZnO, etc. Normally, such transformation in the bulk optical properties of material should be produced by a strong perturbation from the external agent, in this case, the Ag nanoparticles[26]. However, considering the low thickness of the SZN, i.e. approximately 15 nm, bulk electronic modification in the SZN by the Ag nanoparticles attachment would be possible. This certainly is followed by modification of the overall physicochemistry properties of the SZN. Enhanced performance in the existing application is expected from the Ag decorated SZN.

Table 1. Average pore diameter for SZNs prepared at five different concentrations.

Zn Precursor Concentrations (M)	Average Pore Diameter (μm)	Optical band edge (eV)
0.01	1.683	3.310
0.02	1.350	3.305

0.03	0.941	3.290
0.04	0.729	3.290
0.05	0.654	3.290

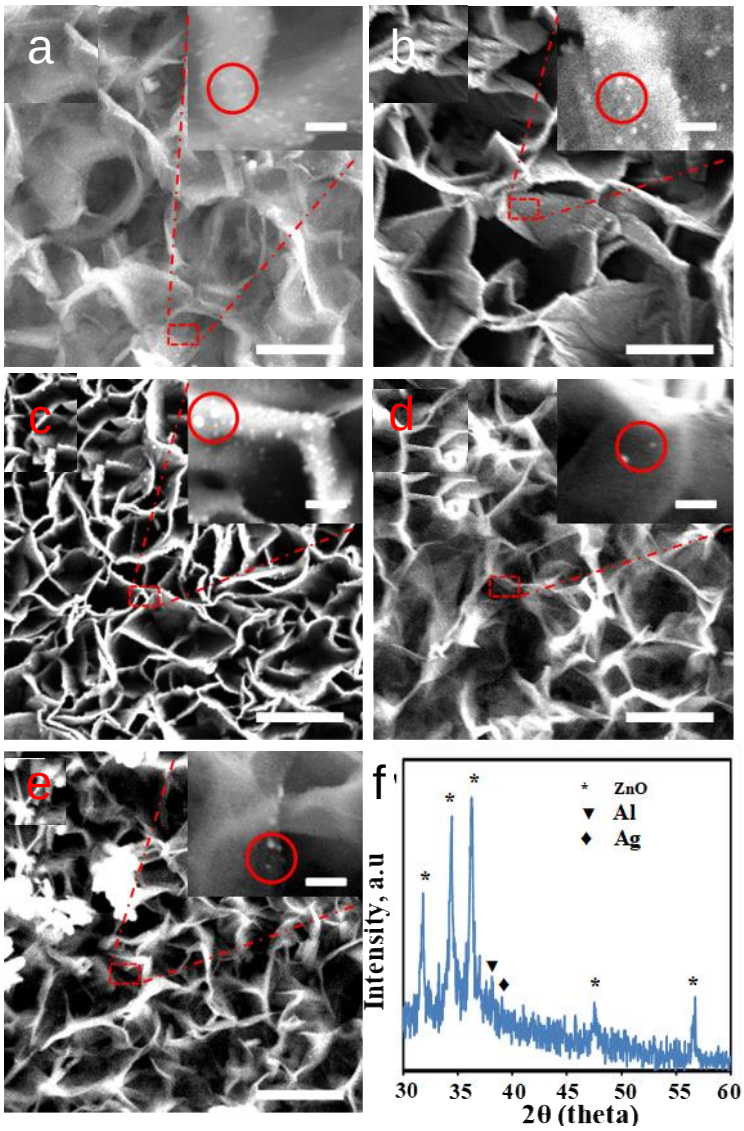

Figure 3. (a-e) FESEM image of vertical ZnO nanosheet from different precursor concentrations as in Figure 1 decorated with Ag nanoparticles. f is the XRD pattern of the sample. Scale bars are 1 μm and 100 nm in the inset.

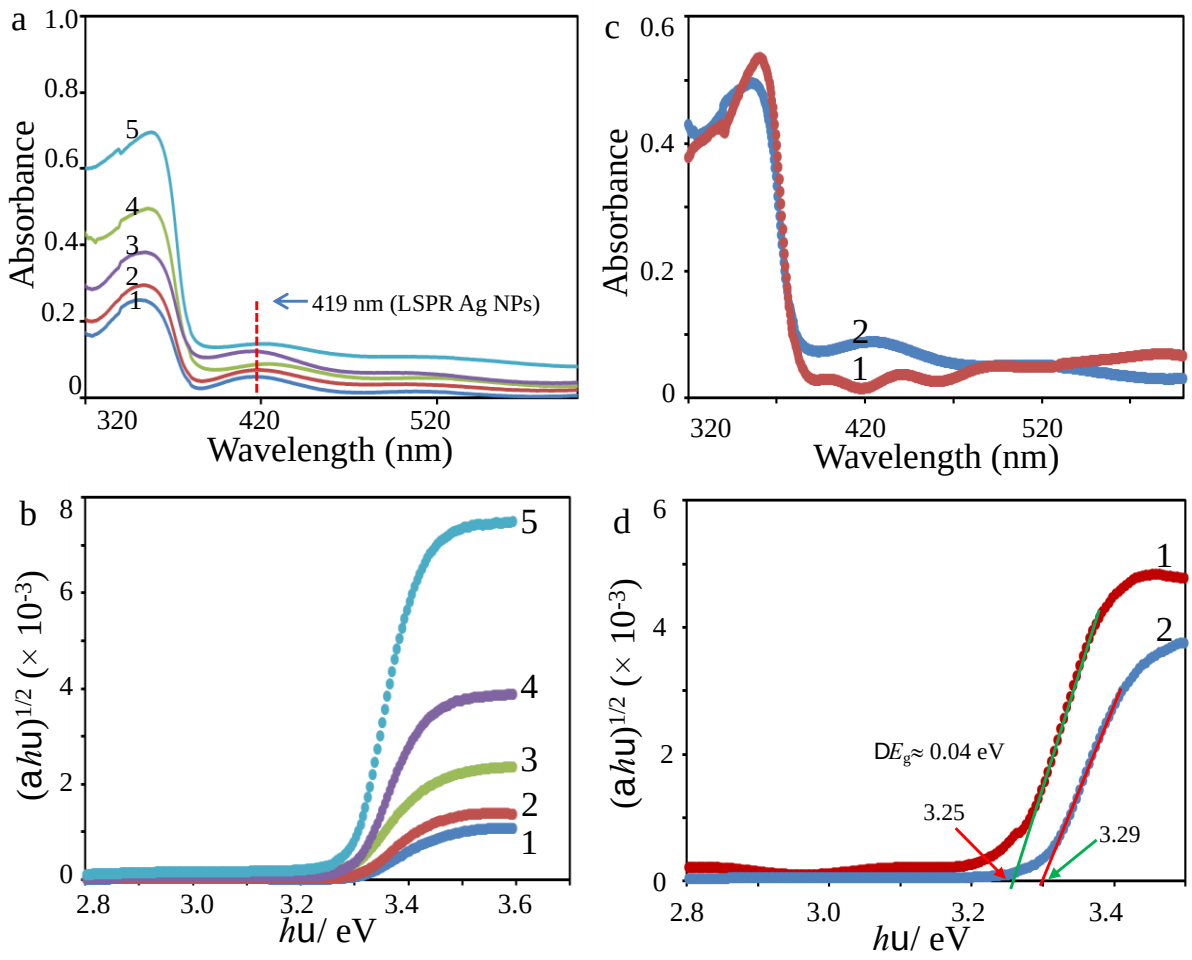

Figure 4. (a) Optical absorbance of the vertical ZnO nanosheet decorated with Ag nanoparticles with different ZnO precursor concentration, i.e. 0.01 (1), 0.02 (2), 0.03 (3), 0.04 (4) and 0.05 M (5). (b) Corresponding Tauc plot of the samples. (c) Comparison of optical absorption properties of pristine ZnO nanosheet (curve 1) and Ag nanoparticles decorated ZnO nanosheet (curve 2) and (d) their corresponding Tauc plot showing modification on the optical bandgap.

We again remark that the Ag nanoparticles have effectively modified the optical properties of SZN, which was achieved via a two-steps process. We predict that, although the present result uses FTO as the substrate, the method should also be extended to grow SZN on other substrates, such as glass. While the two-step method could be a tricky and lengthy process, notwithstanding, it offers a sophisticated way to attain a preserved morphology of the SZN and the Ag nanoparticles. A simple, one-pot reaction process has been used to grow and modify the electrical and optical properties of the ZnO nanostructure as in the formation of Ag-ZnO nanorod[27]. Nevertheless, although it might produce effective modification on

the optical properties of ZnO nanostructure, it may induce a deformation on the two-dimensional crystal growth in the ZnO. Therefore, a special effort could be conducted to realize a one-pot process for the preparation of Ag nanoparticles decorated SZN.

Nevertheless, the Al system is still detected in the sample with significant content as shown in the XRD analysis result. This is the result of the Al layer is not fully consumed during the catalytic growth of SZN. It may certainly generate a strong effect on the optical and electrical properties of the SZN. At this stage, the approach to remove or decrease the Al content in the SZN is not yet obtained. We assumed that the use of appropriate thickness of Al layer or the use of an additional catalyst to accelerate the Al consumption might remove or reduce the Al presence in the SZN. This effort is being pursued and the result will be reported separately.

4. Conclusions

The method to prepare SZN on the substrate surface has been presented via the microwave-assisted hydrothermal method. The standing ZnO nanosheet has a length of up to 1 um and thickness can be as low as 10 nm. We also discovered that the Ag nanoparticles of size up to 20 nm can induce change in the optical absorption properties of the SZN. In the typical process, the optical energy band edge of the SZN blue shifts as high as 0.04 eV upon being decorated with the Ag nanoparticles. This is unusual and is assumed due to the thin structure of the nanosheet so that the Ag nanoparticles attachment on the surface can strongly distort both the surface and the bulk lattice of the SZN. This system should find extensive application in sensors, photocatalysis, and solar cells.

Acknowledgment

The authors thank the Ministry of Higher Education of Malaysia for supporting this project under FRGS/1/2019/STG02/UKM/02/3 grant.

References

[1] S Polarz 2011 *Adv. Funct. Mater.* **21** 3214.

[2] C Burda, X Chen, R Narayanan, MA El-Sayed 2005 *Chem. Rev.* **105** 1025.

[3] A Mclaren, T Valdes-Solis, G Li, SC Tsang 2009 *J. Am. Chem. Soc.* **131** 12540.

[4] AP Alivisatos 1996 *Science* **271** 933.

[5] A Ali Umar, M Oyama 2005 *Cryst. Growth Des.* **5** 599.

[6] A Ali Umar, M Oyama 2006 *Cryst. Growth Des.* **6** 818.

[7] A Ali Umar, M Oyama 2008 *Cryst. Growth Des.* **9** 1146.

[8] A Ali Umar, M Oyama, M Mat Salleh, B Yeop Majlis 2010 *Cryst. Growth Des.* **10** 3694.

[9] R Viswanatha, S Sapra, B Satpati, P Satyam, B Dev, D Sarma 2004 *J. Mater. Chem.* **14** 661.

[10] AL Schoenhalz, JT Arantes, A Fazzio, GM Dalpian 2010 *J. Phys. Chem. C* **114** 18293.

[11] J-H Zhao, C-J Liu, Z-H Lv 2016 *Optik* **127** 1421.

[12] CT Quy, CM Hung, N Van Duy, ND Hoa, M Jiao, H Nguyen 2017 *J. Electron. Mater.* **46** 3406.

[13] N Mintcheva, AA Aljulaih, W Wunderlich, SA Kulinich, S Iwamori 2018 *Materials* **11** 1127.

[14] ST Tan, A Ali Umar, A Balouch, et al. 2014 *ACS Combinat. Sci.* **16** 314.

[15] SFC Orou, KJ Hang, MT Thien, et al. 2018 *J. Ind. Eng. Chem.* **62** 333.

[16] MH Al-Hinai, P Sathe, MZ Al-Abri, S Dobretsov, AT Al-Hinai, J Dutta 2017 *ACS Omega* **2** 3157.

[17] MYA Rahman, A Umar, R Taslim, MM Salleh 2013 *Electrochim. Acta* **88** 639.

[18] ST Tan, AA Umar, MM Salleh 2016 *J. Phys. Chem. Solids* **93** 73.

[19] NJ Ridha, AA Umar, F Alosfur, MHH Jumali, MM Salleh (2013) *J. Nanosci. Nanotechnol.* **13** 2667.

[20] ST Tan, AA Umar, A Balouch, et al. 2014 *Ultrason. Sonochem*. **21** 754.

[21] R Viswanatha, H Amenitsch, D Sarma 2007 *J. Am. Chem. Soc.* **129** 4470.

[22] R Viswanatha, PK Santra, C Dasgupta, D Sarma 2007 *Phys. Rev. Lett*. **98** 255501.

[23] R Laskowski, NE Christensen 2006 *Phys. Rev. B* **73** 045201.

[24] S Nafisah, S Saad, A Umar, et al. 2015 *Optica Applicata* **45** 263

[25] L Miao, S Tanemura, M Tanemura, SP Lau, B Tay 2007 *J. Mater. Sci.: Mater. Electron.* **18** 343.

[26] RM Hewlett, MA McLachlan 2016 *Adv. Mater.* **28** 3893.

[27] S Sarkar, D Basak 2013 *CrystEngComm* **15** 7606.

Synthesis of standing ZnO nanosheets and impact of Ag nanoparticles loading on its optical property

Marjoni Imamora Ali Umar*[1,*], Setia Budi[2], Muhammad Nurdin[3], and Akrajas Ali Umar*[4]

[1]Faculty of Tarbiyah, Department of Physical Education, Faculty of Tarbiyah, Insitut Agama Islam Negeri Batusangkar, Batu Sangkar, 27213 West Sumatera, Indonesia.

[2]Faculty of Mathematics and Natural Science, Department of Chemistry, Faculty of Mathematics and Natural Science, Universitas Negeri Jakarta, 13220 DKI Jakarta 13220, Indonesia.

[3]Faculty of Mathematics and Natural Science, Department of Chemistry, Faculty of Mathematics and Natural Science, Universitas Halu Oleo, Kendari, 93232 South East Sulawesi, Indonesia.

[4]Institute of Microengeineering and Nanoelectronics, Universiti Kebangsaan Malaysia, 43600 UKM Bangi 43600, Selangor, Malaysia.

*Corresponding Author:Author for correspondence (marjoniimamora@gmail.com (MIAU), akrajas@ukm.edu.my (AAU).

Abstract

Anisotropic nanostructures, such as nanosheets, nanorods, etc., in many cases, generate superior physicochemical properties over a highly symmetric structure counterpart. Here, we present a straightforward method to grow vertically oriented ZnO nanosheet directly on fluorine-tin oxide substrate using a microwave-assisted quasi-hydrothermal method. We also found that the Ag nanoparticles (AgNPs) loading on the surface can effectively modify their optical properties, the potential for upgrading its performance in the existing applications.

Commented [NK1]: Only one corresponding author may be listed on the article in the event of publication. Whoever is designated as a corresponding author in the submission system will be listed as such upon publication.

Formatted: Superscript

Due to the simplicity of the technique, AgNP~~Ag nanoparticle~~s ~~-~~loaded standing ZnO nanosheet should find potential application in solar cells, sensing~~,~~ and photocatalysis.

Keywords: Standing nanosheets; ZnO nanostructure; Ag nanoparticles; microwave-assisted hydrothermal.

1. Introduction

The morphology of the nanocrystals gives a strong influence on the overall properties of the materials [1-3]. This is the result of the modification of the confinement potential of the charge carrier when the shape of the nanocrystals is distorted under the quantum regime [4]. For example, ~~for~~ in the case of Au or Ag nanoparticles (AgNPs), their surface plasmonic resonance changes from single localized surface resonance to two localized surface plasmon resonance characters, when their morphology transformed from spherical nanoparticles to nanorods or nanoplates morphology [5-8]. A similar case is also encountered in the ZnO nanocrystals [9,~~-~~10]. For example, its excitonic photoluminescence properties redshifted from 369 ~~nm~~ to 371 nm when its morphology altered from spherical to nanorods, respectively [11]. Not only excitonic-related photoluminescence shift but also the nature of defect-related photoluminescence, i.e., blueshifted from 528 ~~nm~~ to 514 nm when the nanostructure shape changes from spherical to nanorods, respectively. In addition, owing to the alteration of the surface atom when the morphology of the nanostructure changes, their surface physicochemical properties are strongly transformed. This results in the enhancement of the surface reactivity in sensing [12], photocatalysis [13,~~-~~14], surface biological activity [15,~~-~~16]~~,~~ and solar cells [17] when the morphology of ZnO nanostructure is modified from highly symmetrical spherical morphology to anisotropic shapes, such as nanorods, nanoplates, etc. [18]. Considering the nature of physicochemistry transformation under morphology shift, the attempt to continuously prepare ZnO nanostructure with exotic anisotropic morphology should be demonstrated.

In this study, a simple and rapid method to grow a standing nanosheet of ZnO directly on the substrate surface is demonstrated via a microwave-assisted quasi-hydrothermal method [19]. In the typical process, the standing nanosheet has a length up to 1 μm and the thickness of the nanosheet is approximately 10 nm. The nanosheet growth direction on the surface is random, producing a pore-like surface, the result of the nanosheet network on the surface. We also found that the optical property of the standing ZnO nanosheet (SZN) significantly

modified upon being decorated with AgNP~~Ag nanoparticle~~s of size from 15 to 20 nm on their surface, which is hardly achieved in other systems such as nanorods or other morphologies. An optical energy gap red-shifting up to 0.04 eV was observed, signifying its potential for improved photo-activity properties in the application. The AgNP~~Ag nanoparticle~~s loaded standing nanosheet of ZnO may find use in solar cells and non-linear optics applications.

2. Experimental

2.1~~.~~ ~~Ag nanoparticles (~~AgNPs~~)~~-loaded ~~standing ZnO nanosheet~~SZN ~~(Ag-SZN)~~ preparation~~.~~

AgNPs-loaded ~~standing ZnO nanosheet~~SZN (Ag-SZN) on a fluorine-doped indium tin oxide (FTO) substrate were prepared by a two-step process, i.e., SZN growth and AgNPs loading onto the SZN structure. The SZN on FTO substrate (Sigma-Aldrich, the sheet resistance of ca. 10 Ω per ~~/~~square) was prepared by using our previously reported technique, namely microwave-assisted hydrolysis seed-mediated growth process [19]. Briefly, a cleaned FTO substrate that has been undergone a standard cleaning process in acetone and ethanol under an ultrasonication was sputtered with a thin layer of Al film (thickness approximately 30 nm) using an RF Magnetron Sputter machine. After following a further brief-cleaning process under ultrasonication in ethanol, ZnO nanoseeds of size approximately from 3 to 10 nm were deposited on the Al layer using alcohothermal seeding method [20], namely consecutive spin-coating of ethanolic solution of zinc nitrate hydrate, $ZnNO_3 \cdot 6H_2O$ (Alfa Aesar) and thermal annealing (using a split-tube furnace system (Thermcraft, USA)) at 200 °C in air for 1 h. The SZN was then grown by simply immersing the FTO/Al-loaded ZnO nanoseed substrate into a growth solution that contains an equimolar (0.3 M) aqueous solution of $ZnNO_3 \cdot 6H_2O$ and 0.03 M hexamethylene tetramine~~hexamethytetramine (HMT)~~. The growth reaction was carried out under microwave irradiation (power ca. ~1100 W) inside a microwave oven (Panasonic) for 20 s. The sample was then taken out, washed in a copious amount of pure water, and dried using a flow of nitrogen gas. The ~~as~~ as-prepared SZNs were then annealed for 1 h in the air at 350 °C to remove any organic residue on the sample and to obtain a better ZnO crystallinity. From this procedure, a high-density SZN structure on the FTO substrate (confirmed by X-ray diffraction (XRD) and field emission scanning electron microscopy (FESEM) results) was~~ill be~~ obtained. In this study, the SZN with five different porous densities were prepared by simply varying the Zn precursor ($ZnNO_3 \cdot 6H_2O$) concentrations in the reaction, namely 0.01, 0.02, 0.03, 0.04~~,~~ and 0.05 M. Other reagents and procedures used in this work were kept unchanged.

Commented [NK2]: Check and confirm 'hexamethytetramine' has been changed to 'hexamethylene tetramine'

The Ag nanoparticle (AgNPs)-loaded SZN (Ag-SZN) were prepared by firstly immersing the SZN-coated FTO substrate into a 20 ml aqueous solution that contains 0.5 ml of 0.01 M $AgNO_3$ (Sigma-Aldrich, USA) and 0.5 ml of 0.01 M trisodium citrate (WAKO Chemical, Japan). The sample was left for 30 min undisturbed to facilitate Ag^+ ions adsorption onto the SZN surface. After that, 0.1 ml of ice-cooled $NaBH_4$ (0.1 M) was injected into the solution. The colour of the solution changed from colourless to yellow, indicating the formation of Ag both in the solution and on the surface of SZN. The reaction was then left undisturbed for another 1.5 h at room temperature, to facilitate the effective growth of Ag ~~nanoparticle~~NPs on the surface of SZN. The sample was then taken out, washed with a copious amount of pure water, and finally dried with a flow of nitrogen gas. Finally, the sample was annealed in air at 200 °C for 1 h to remove any organic residue on the sample surface.

2.2. Characterizations

The morphologies of the unloaded and Ag-SZN were obtained using a field emission scanning electron microscopy (FESEM) Zeiss Supra 55VP FESEM apparatus. The phase and structural properties of the unloaded and Ag-SZN were characterized by X-ray diffraction (XRD) measurements using Bruker D8Advance with CuKα radiation (λ = 1.541 Å) and scan rate as low as 2° min^{-1}. UV-Vis diffuse reflectance spectroscopy (Winlab, Hitachi, Japan) was used to obtain the optical properties of the sample.

3. Results and discussion

3.1 AgNP ~~nanoparticle~~ loaded SZN

Standing ZnO nanosheet ~~(SZN)~~ with controlled porous density on the FTO substrate surface has been successfully prepared using the present method. Figure 1 shows the typical surface morphology of the SZN grown using five different Zn precursor concentrations, namely 0.01, 0.02, 0.03, 0.04~~,~~ and 0.05 M. As shown in figure 1 ~~reveals~~, the SZN is characterized by a continuously connected nanosheet structure that is vertically grown on the substrate surface, forming a porous surface structure. The thickness of the nanosheet is in the range of 10 ~~to~~ 15 nm and was found to have no significant dependency on the Zn precursors concentration used in the reaction. However, the pore size (the average edge-to-edge

Formatted: Superscript

Formatted: Font: Italic

Formatted: Superscript

distance) decreases with the increase of ZnO precursor concentration in the reaction. For example, at low concentration (see figure 1a), the size of the pore is approximately 500 nm. The pore size effectively decreases when the precursor concentration was increased (figure 1a–e). At a relatively high concentration, i.e., 0.05 M (see figure 1 e), the pore size is as low as ca. 50 nm. This produces SZN with high-pore density on the substrate surface, promising unique optical and electrical properties. A complete porosity data of nanosheet film grown from different ZnO precursor concentrations is summarized in table 1. The increase ing of the pore density upon the increasing of ZnO precursor concentration is simply related to the high-kinetic nature of the growth reaction at high precursor concentration, causing rapid growth and deposition of the ZnO nanostructure onto the surface [21,-22]. Therefore, at this condition, the competitive nucleation characteristic of the reaction is high, resulting in the formation of smaller pore size, thus increases the density. Unfortunately, as can be seen from the figure, the use of high ZnO precursor concentration has caused un-stability in the reaction that was indicated by an active formation of ZnO by-product in solution (ZnO nanorods), of which some of them are attached to the nanosheet surface. This could more or less distort the unique property of the porous nanosheet film. The results are shown in figures 1e and 1f (it's a magnified images).

The formation of nanosheet structure has been understood as the effect of effective etching and passivation of (101) and (100) planes by the Al-$(OH)_4^-$ complexes in the solution that is produced from the dissolution of the Al layer by hexamethylene tetramine [19]. This condition favours the growth of two-dimensional morphology instead of other morphologies, such as spherical or irregular shape nanostructures.

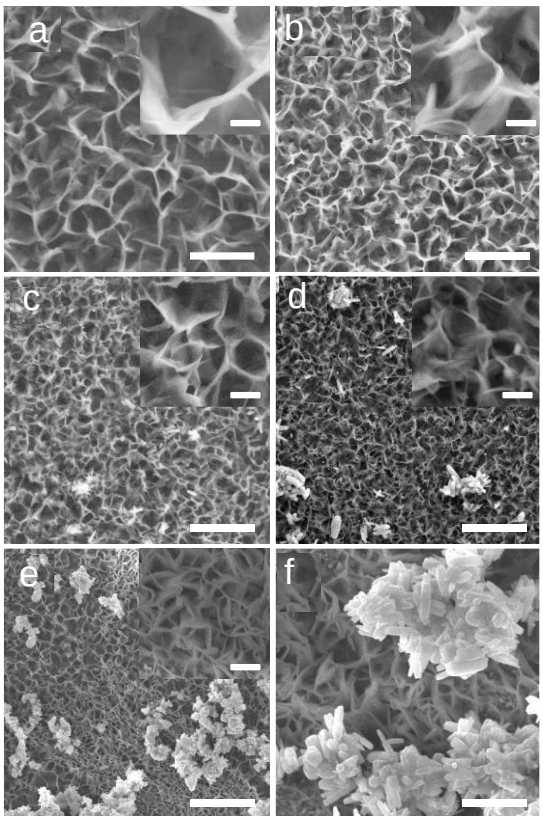

Figure 1. FESEM micrograph for ~~PZNs~~ SZNs morphology at various Zn^{+} precursor molarities, namely (**a**) 0.01, (**b**) 0.02, (**c**) 0.03, (**d**) 0.04~~,~~ and (**e**) 0.05 M. (**f**) ~~shows a~~A high magnification image for sample **e**. Scale bars are 1 µm and 100 nm for insets and **f**.

Figure 2 shows the phase analysis result of the SZN that were prepared using five different Zn^{+} precursor solutions, namely 0.01, 0.02, 0.03, 0.04~~,~~ and 0.05 M. As can be seen from the figure, the entire sample shows a similar XRD pattern with the presence of five major peaks in the spectrum, namely at 2θ of 31.6, 34.3, 36.2, 47.5 and 56.6°. This XRD pattern agrees well with the standard XRD ~~diffraction~~ data (file no. 36-1451) for the pure ZnO phase with peaks at 2θ of 31.6, 34.3, 36.2, 47.5~~,~~ and 56.6° corresponding to the XRD ~~diffraction~~ from the (100), (002), (101) (102), and (111) Bragg planes, respectively. It can be

Formatted: Superscript
Formatted: Font: Bold
Formatted: Font: Bold
Formatted: Font: Bold
Formatted: Font: Bold
Formatted: Font: Bold
Formatted: Font: Bold
Formatted: Font: Bold
Formatted: Font: Bold
Formatted: Superscript
Formatted: Font: Italic
Formatted: Font: Italic

noted here that the SZN produce from the lower precursor concentration seems to be characterized by the (002) plane (*c*-axis plane) because of a high-diffraction intensity originated from this plane (see curve *a*). However, the XRD profile was effectively modified when the SZN was prepared using a higher ZnO precursor concentration (see curves *b* to *e*). At these concentrations, the SZNs were characterized by (101) plane with ratio diffraction intensity between (101) and (002) planes as high as 1.5, which is only 0.5 for sample *a*. It is also observed that the diffraction from the (100) plane is also high and comparable to the (002) plane with an intensity ratio between (100) and (002) in the range of 0.6 to 0.8, which is only 0.4 for the sample *a*. We assumed that the SZN wall should be characterized by the planes of (101) and (100) ~~planes~~. As the (101) and (100) planes for ZnO is a highly energetic surface, thus we expect peculiar optical and electrical properties ~~can~~ to be produced from this structure. In addition, from the spectra, the Al crystal peaks were also present, namely at 38.0° and 56.5°. This could be from the Al layer that is not completely consumed during the SZN formation. However, their intensity is relatively low and its effect on the optical and electrical properties of SZN ~~are~~ is expected to be minimum.

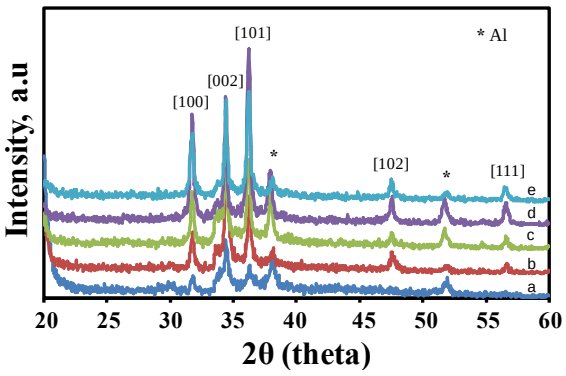

Figure 2. XRD spectra for ~~PZNs~~ SZNs morphology at various Zn^{+} precursor molarities of (a) 0.01, (b) 0.02 ~~and~~, (c) 0.03, (d) 0.04 and (e) 0.05 M. ~~shown respectively.~~

We then grew Ag ~~nanoparticle~~NPs onto the surface of SZN by our previously reported technique that involves a simple immersion of the SZN sample into the solution of Ag colloidal reaction formation. After finishing the AgNP ~~nanoparticle~~ growth procedure for 1.5 h and followed by brief rinsing using pure water, we carried out a FESEM analysis to confirm the Ag ~~nanoparticle~~NPs formation on the SZN surface. The result is shown in figure

Formatted: Font: Italic
Formatted: Font: Italic
Formatted: Font: Italic
Formatted: Font: Italic
Formatted: Font: Italic
Formatted: Superscript

3. As shown in figure 3 ~~shows~~, the AgNP ~~nanoparticle~~s have been effectively attached to the surface of the SZN. They are indicated as bright dotted particles as shown in the high-resolution FESEM image in the inset of the corresponding FESEM image (see figure 3a ~~–~~e). Their size range from 15 to 20 nm. The elemental analysis using electron energy dispersion spectroscopy (EDS) might further verify the AgNP ~~nanoparticle~~s existence on the surface of SZN. Nevertheless, due to the limited access to the technique, we cannot provide them at this stage. However, the presence of such bright nanoparticles on the surface of SZN after a treatment in the AgNP ~~nanoparticle~~s colloidal reaction is a clear indication that the Ag ~~nanoparticle~~NPs successfully decorate the SZN. Notwithstanding, the XRD and optical absorption analys~~e~~is (will be discussed in the following) ha~~ve~~s confirmed that the AgNP ~~nanoparticle~~s are existing in SZN thin films.

We then performed an XRD analysis of the sample to further verify the existence of the Ag ~~nanoparticle~~NPs in the sample. A sample with medium Zn precursor concentration, i.e., 0.03 M, was used in the analysis. As has been expected, the Ag crystalline phase is observed in the XRD spectrum along with the ZnO and Al (see figure 3f). The SZN decorated with AgNPs ~~nanoparticles~~ should produce special properties so that unusually high performance in the application would be obtained. As shown in ~~the~~ figure ~~reveals~~, the peak intensity of the Ag ~~nanoparticle~~NPs is indeed weak if compared even with the Al. Because the XRD peak intensity is related to the crystallite size ratio of the component in the sample where SZN, particularly, majorly composes the sample, the diffraction peaks are dominated by the SZN leaving other crystallite components weakly observed in the XRD pattern. The Al peak intensity is higher than the Ag ~~nanoparticle~~NPs, which could be due to the same reason where Al layer crystallite size is bigger than AgNP ~~nanoparticle~~s. It is because Al layer is not completely consumed during the catalytic projection of SZN. The Al layer was deposited on the entire surface of the substrate with a thickness of approximately 30 nm. An incomplete consumption of Al layer during the growth of SZN could leave the Al layer with crystallite size higher than Ag ~~nanoparticle~~NPs (size approximately 15 nm). Thus, the Al layer XRD peak is higher than AgNP ~~nanoparticle~~s.

We ~~then~~ carried out a UV-Vis absorption spectroscopy technique to further verify the presence of Ag ~~nanoparticle~~NPs on the surface of SZN and to evaluate~~d~~ the optical properties of the SZN under the influence of Ag ~~nanoparticle~~NPs attachment. Figure 4a shows their corresponding optical absorbance. It is seen that excitonic absorption of ZnO (at the wavelength of ca. 360 nm) [23] along with localized surface plasmon resonance absorption of Ag (ca. 419 nm) [24] are observed in the spectrum. This certainly is a further confirmation of

the Ag ~~nanoparticle~~NP''s existence on the surface of SZN. As can be seen from figure 4b and table 1, it can be estimated that there is a modification in the optical bandgap of the SZN when its dimension is altered due to the dimensional effect at this nanostructure regime or decorated with the Ag ~~nanoparticle~~NP. We then extrapolate the Tauc plot from the absorbance spectrum of the sample to see the impact of dimension modification and the Ag ~~nanoparticle~~NP attachment on the optical properties of the SZN (see figure 4b). For example, the thinnest SZN (curve 1 in figure 4b) decorated with the Ag ~~nanoparticle~~NPs has an optical band edge as high as 3.31 eV. It gradually decreases with the increase of thickness and has an optical energy gap as low as 3.29 eV in the thick~~n~~es~~t~~s ZnO nanosheet (curve 5 in figure 4b). Because the Ag ~~nanoparticle~~NPs dimension and density on the SZN surface are more or less similar on each SZN sample, as expected, we can remark that the energy gap decrease should be due to the increase in~~g of~~ SZN dimension and thickness [25]. To understand the extent effect of Ag ~~nanoparticle~~NP impact on the optical properties of the ~~standing ZnO nanosheet~~SZN, we compared the optical properties of pristine SZN~~standing ZnO nanosheet~~ with the ones decorated with Ag ~~nanoparticle~~NPs that were prepared using similar ZnO precursor concentration (0.04 M). The result is shown in figure~~s~~ 4c and d. We noticed that the band edge of the ZnO is blue-shifted up to 0.04 eV with the attachment of Ag ~~nanoparticle~~NPs (figure 4d). The pristine SZN optical band edge is approximately 3.25 eV. This result is quite surprising as surface attachment of the Ag ~~nanoparticle~~NPs in fact can induce the bulk optical properties of the SZN, which could be via many ways such as carrier equilibration effect, Fermi level alignment between the Ag and ZnO, etc. Normally, such transformation in the bulk optical properties of material should be produced by a strong perturbation from the external agent, in this case, the Ag ~~nanoparticle~~NPs [26]. However, considering the low thickness of the SZN, i.e., approximately 15 nm, bulk electronic modification in the SZN by the Ag ~~nanoparticle~~NPs attachment would be possible. This certainly is followed by modification of the overall physicochemistry properties of the SZN. Enhanced performance in the existing application is expected from the Ag ~~-~~decorated SZN.

Table 1. Average pore diameter for SZNs prepared at five different concentrations.

Zn precursor concentrations (M)	Average pore diameter (μm)	Optical band edge (eV)
0.01	1.683	3.310

0.02	1.350	3.305
0.03	0.941	3.290
0.04	0.729	3.290
0.05	-0.654	3.290

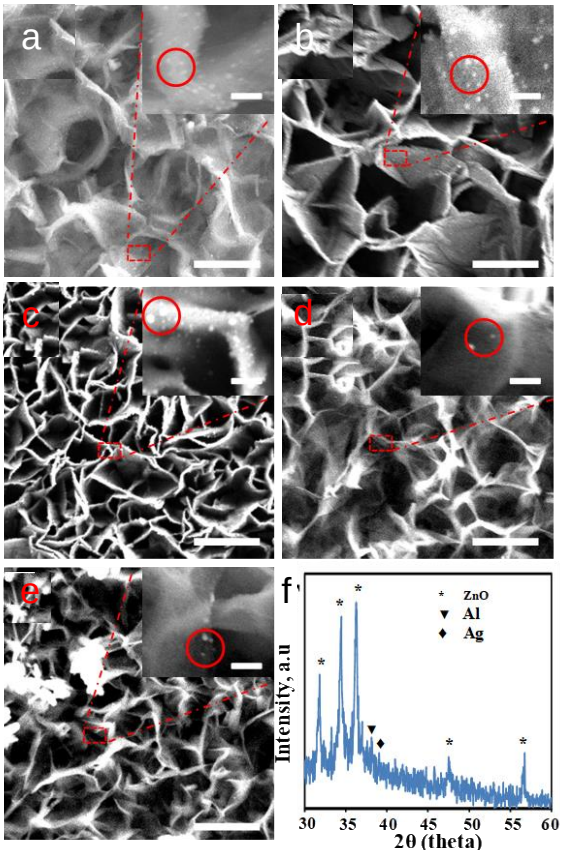

Figure 3. (**a**–**e**) FESEM image of vertical ZnO nanosheet from different precursor concentrations, as in figure 1, decorated with Ag ~~nanoparticle~~NPs. Panel **f** is the XRD pattern of the sample. Scale bars are 1 μm and 100 nm in the inset.

Formatted: Font: Bold

Formatted: Font: Bold

Formatted: Font: Bold

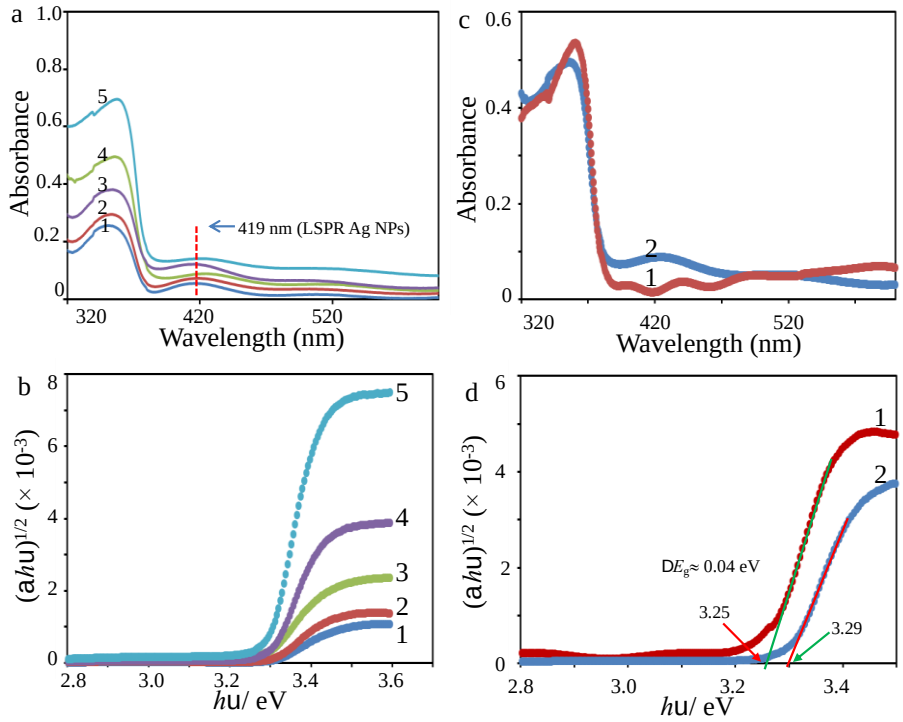

Figure 4. (**a**) Optical absorbance of the vertical ZnO nanosheet decorated with Ag ~~nanoparticle~~NPs with different ZnO precursor concentrations, i.e., 0.01 (1), 0.02 (2), 0.03 (3), 0.04 (4) and 0.05 M (5). (**b**) Corresponding Tauc plot of the samples. (**c**) Comparison of optical absorption properties of pristine ZnO nanosheet (curve 1) and Ag-~~nanoparticle~~NPs decorated ZnO nanosheet (curve 2), and (**d**) their corresponding Tauc plot showing modification on the optical bandgap.

Formatted: Font: Bold

Formatted: Font: Bold

Formatted: Font: Bold

Formatted: Font: Bold

We again remark that the Ag-~~nanoparticle~~NPs have effectively modified the optical properties of SZN, which was achieved via a two-step~~s~~ process. We predict that, although the present result uses FTO as the substrate, the method should also be extended to grow SZN on other substrates, such as glass. While the two-step method could be a tricky and lengthy process, notwithstanding, it offers a sophisticated way to attain a preserved morphology of the SZN and the Ag-~~nanoparticle~~NPs. A simple, one-pot reaction process has been used to grow and modify the electrical and optical properties of the ZnO nanostructure as in the formation of Ag-ZnO nanorod [27]. Nevertheless, although it might produce effective

modification on the optical properties of ZnO nanostructure, it may induce a deformation on the two-dimensional crystal growth in the ZnO. Therefore, a special effort could be conducted to realize a one-pot process for the preparation of Ag ~~nanoparticle~~NPs ~~-~~decorated SZN.

Nevertheless, the Al system is still detected in the sample with significant content as shown in the XRD analysis result. This is the result of the Al layer that is not fully consumed during the catalytic growth of SZN. It may certainly generate a strong effect on the optical and electrical properties of the SZN. At this stage, the approach to remove or decrease the Al content in the SZN is not yet obtained. We assumed that the use of appropriate thickness of Al layer or the use of an additional catalyst to accelerate the Al consumption might remove or reduce the Al presence in the SZN. This effort is being pursued and the result will be reported separately.

4. Conclusions

The method to prepare SZN on the substrate surface has been presented via the microwave-assisted hydrothermal method. The SZN~~standing ZnO nanosheet~~ has a length of up to 1 μ~~u~~m and thickness can be as low as 10 nm. We also discovered that the Ag ~~nanoparticle~~NPs of size up to 20 nm can induce change in the optical absorption properties of the SZN. In the typical process, the optical energy band edge of the SZN blue shifts as high as 0.04 eV upon being decorated with the Ag ~~nanoparticle~~NPs. This is unusual and is assumed due to the thin structure of the nanosheet so that the Ag ~~nanoparticle~~NPs attachment on the surface can strongly distort both the surface and the bulk lattice of the SZN. This system should find extensive application in sensors, photocatalysis~~,~~ and solar cells.

Acknowledgment

~~The authors~~We thank the Ministry of Higher Education of Malaysia, for supporting this project under FRGS/1/2019/STG02/UKM/02/3 grant.

References

[1] Polarz S 2011 *Adv. Funct. Mater.* **21** 3214~~.~~

[2] Burda C, ~~X~~ Chen X, ~~R~~ Narayanan R and~~,~~ ~~MA~~ El-Sayed M A 2005 *Chem. Rev.* **105** 1025~~.~~

[3] A Mclaren A, T Valdes-Solis T, G Li G and, SC Tsang S C 2009 *J. Am. Chem. Soc.* **131** 12540.

[4] AP Alivisatos A P 1996 *Science* **271** 933.

[5] A Ali Umar A and, M Oyama M 2005 *Cryst. Growth Des.* **5** 599.

[6] A Ali Umar A, and M Oyama M 2006 *Cryst. Growth Des.* **6** 818.

[7] A Ali Umar A and, M Oyama M 2008 *Cryst. Growth Des.* **9** 1146.

[8] A Ali Umar A, M Oyama M, M Mat Salleh M and, B Yeop Majlis B 2010 *Cryst. Growth Des.* **10** 3694.

[9] R Viswanatha R, S Sapra S, B Satpati B, P Satyam P, B Dev B and, D Sarma D 2004 *J. Mater. Chem.* **14** 661.

[10] AL Schoenhalz A L, JT Arantes J T, A Fazzio A and, GM Dalpian G M 2010 *J. Phys. Chem. C* **114** 18293.

[11] J H Zhao J-H, C J Liu C-J, and Z H Lv Z-H 2016 *Optik* **127** 1421.

[12] CT Quy C T, CM Hung C M, N Van Duy N, ND Hoa N D, M Jiao M and, H Nguyen H 2017 *J. Electron. Mater.* **46** 3406.

[13] N Mintcheva N, AA Aljulaih A A, W Wunderlich W, SA Kulinich S A, S Iwamori S 2018 *Materials* **11** 1127.

[14] ST Tan S T, A Ali Umar A, A Balouch A, Yahaya M, Yap C C, Salleh M M *et al.* 2014 *ACS Combinat. Sci.* **16** 314.

[15] SFC Orou S F C, KJ Hang K J, MT Thien M T, Ying Y L, Diem N D N, Goh B H *et al.* 2018 *J. Ind. Eng. Chem.* **62** 333.

[16] MH Al-Hinai M H, P Sathe P, MZ Al-Abri M Z, S Dobretsov S, AT Al-Hinai A T and, J Dutta J 2017 *ACS Omega* **2** 3157.

[17] MYA Rahman M Y A, A Umar A, R Taslim R and, MM Salleh M M 2013 *Electrochim. Acta* **88** 639.

[18] ST Tan S T, AA Umar A A and, MM Salleh M M 2016 *J. Phys. Chem. Solids* **93** 73.

[19] NJ Ridha N J, AA Umar A A, F Alosfur F, MHH Jumali M H H and, MM Salleh M M (2013) *J. Nanosci. Nanotechnol.* **13** 2667.

[20] ST Tan S T, AA Umar A A, A Balouch A, Yahaya M, Yap C C, Salleh M M, Oyama, M *et al.* 2014 *Ultrason. Sonochem.* **21** 754.

[21] R Viswanatha R, H Amenitsch H and, D Sarma D 2007 *J. Am. Chem. Soc.* **129** 4470.

[22] R Viswanatha R, PK Santra P K, C Dasgupta C and, D Sarma D 2007 *Phys. Rev. Lett.* **98** 255501.

Formatted: Font: Italic

Formatted: Font: Italic

Formatted: Font: Italic

[23] R Laskowski R and, NE Christensen N E 2006 *Phys. Rev. B* **73** 045201.

[24] S Nafisah S, S Saad S, A Umar A A, Plucinski K, Lis M, Maciaga A *et al.* 2015 *Optica Opt. Applicata Appl.* **45** 263

[25] L Miao L, S Tanemura S, M Tanemura M, SP Lau S P and, B Tay B 2007 *J. Mater. Sci.: Mater. Electron.* **18** 343.

[26] RM Hewlett R M and, MA McLachlan M A 2016 *Adv. Mater.* **28** 3893.

[27] S Sarkar S and, D Basak D 2013 *CrystEngComm.* **15** 7606.

Formatted: Font: Italic

Date:	08/12/2021
To:	"Marjoni Imamora Ali Umar" marjoni.imamora@iainbatusangkar.ac.id
From:	"Amitava Patra" msap@iacs.res.in
Subject:	BOMS: Your manuscript entitled Synthesis of standing ZnO nanosheets and impact of Ag nanoparticles loading on its optical property

Ref.:
Ms. No. BOMS-D-21-00755R1
Synthesis of standing ZnO nanosheets and impact of Ag nanoparticles loading on its optical property
Bulletin of Materials Science

Dear Dr Ali Umar,

I am pleased to tell you that your work has now been accepted for publication in Bulletin of Materials Science.

Thank you for submitting your work to this journal.

With kind regards

Amitava Patra, Ph.D
Associate Editor
Bulletin of Materials Science

****

Our flexible approach during the COVID-19 pandemic

If you need more time at any stage of the peer-review process, please do let us know. While our systems will continue to remind you of the original timelines, we aim to be as flexible as possible during the current pandemic.

This letter contains confidential information, is for your own use, and should not be forwarded to third parties.

Recipients of this email are registered users within the Editorial Manager database for this journal. We will keep your information on file to use in the process of submitting, evaluating and publishing a manuscript. For more information on how we use your personal details please see our privacy policy at https://www.springernature.com/production-privacy-policy. If you no longer wish to receive messages from this journal or you have questions regarding database management, please contact the Publication Office at the link below.

Bull. Mater. Sci. _####################_
https://doi.org/10.1007/s12034-021-02563-7

Synthesis of standing ZnO nanosheets and impact of Ag nanoparticles loading on its optical property

MARJONI IMAMORA ALI UMAR[1,*], SETIA BUDI[2], MUHAMMAD NURDIN[3] and AKRAJAS ALI UMAR[4]

[1]Faculty of Tarbiyah, Department of Physical Education, Insitut Agama Islam Negeri Batusangkar, Batu Sangkar 27213, Indonesia

[2]Faculty of Mathematics and Natural Science, Department of Chemistry, Universitas Negeri Jakarta, DKI, Jakarta 13220, Indonesia

[3]Faculty of Mathematics and Natural Science, Department of Chemistry, Universitas Halu Oleo, Kendari 93232, Indonesia

[4]Institute of Microengeineering and Nanoelectronics, Universiti Kebangsaan Malaysia, UKM, 43600 Bangi, Malaysia

*Author for correspondence (marjoniimamora@gmail.com)

MS received 15 June 2021; accepted 12 August 2021

Abstract. Anisotropic nanostructures, such as nanosheets, nanorods, etc., in many cases, generate superior physicochemical properties over a highly symmetric structure counterpart. Here, we present a straightforward method to grow vertically oriented ZnO nanosheet directly on fluorine-tin oxide substrate using a microwave-assisted quasi-hydrothermal method. We also found that the Ag nanoparticles (AgNPs) loading on the surface can effectively modify their optical properties, the potential for upgrading its performance in the existing applications. Due to the simplicity of the technique, AgNPs-loaded standing ZnO nanosheet should find potential application in solar cells, sensing and photocatalysis.

Keywords. Standing nanosheets; ZnO nanostructure; Ag nanoparticles; microwave-assisted hydrothermal.

1. Introduction

The morphology of the nanocrystals gives a strong influence on the overall properties of the materials [1–3]. This is the result of the modification of the confinement potential of the charge carrier when the shape of the nanocrystals is distorted under the quantum regime [4]. For example, in the case of Au or Ag nanoparticles (AgNPs), their surface plasmonic resonance changes from single localized surface resonance to two localized surface plasmon resonance characters, when their morphology transformed from spherical nanoparticles to nanorods or nanoplates morphology [5–8]. A similar case is also encountered in the ZnO nanocrystals [9,10]. For example, its excitonic photoluminescence properties redshifted from 369 to 371 nm when its morphology altered from spherical to nanorods, respectively [11]. Not only excitonic-related photoluminescence shift but also the nature of defect-related photoluminescence, i.e., blueshifted from 528 to 514 nm when the nanostructure shape changes from spherical to nanorods, respectively. In addition, owing to the alteration of the surface atom when the morphology of the nanostructure changes, their surface physicochemical properties are strongly transformed. This results in the enhancement of the surface reactivity in sensing [12], photocatalysis [13,14], surface biological activity [15,16] and solar cells [17] when the morphology of ZnO nanostructure is modified from highly symmetrical spherical morphology to anisotropic shapes, such as nanorods, nanoplates, etc. [18]. Considering the nature of physicochemistry transformation under morphology shift, the attempt to continuously prepare ZnO nanostructure with exotic anisotropic morphology should be demonstrated.

In this study, a simple and rapid method to grow a standing nanosheet of ZnO directly on the substrate surface is demonstrated via a microwave-assisted quasi-hydrothermal method [19]. In the typical process, the standing nanosheet has a length up to 1 μm and the thickness of the nanosheet is approximately 10 nm. The nanosheet growth direction on the surface is random, producing a pore-like surface, the result of the nanosheet network on the surface. We also found that the optical property of the standing ZnO nanosheet (SZN) significantly modified upon being decorated with AgNPs of size from 15 to 20 nm on their surface, which is hardly achieved in other systems such as nanorods or other morphologies. An optical energy gap red-shifting up to 0.04 eV was observed, signifying its potential for improved photoactivity properties in the application. The AgNPs loaded standing nanosheet of ZnO may find use in solar cells and non-linear optics applications.

2. Experimental

2.1 *AgNPs-loaded SZN preparation*

AgNPs-loaded SZN (Ag-SZN) on a fluorine-doped indium tin oxide (FTO) substrate were prepared by a two-step process, i.e., SZN growth and AgNPs loading onto the SZN structure. The SZN on FTO substrate (Sigma-Aldrich, the sheet resistance of ca. 10 Ω per square) was prepared by using our previously reported technique, namely microwave-assisted hydrolysis seed-mediated growth process [19]. Briefly, a cleaned FTO substrate that has been undergone a standard cleaning process in acetone and ethanol under an ultrasonication was sputtered with a thin layer of Al film (thickness approximately 30 nm) using an RF Magnetron Sputter machine. After following a further brief-cleaning process under ultrasonication in ethanol, ZnO nanoseeds of size approximately from 3 to 10 nm were deposited on the Al layer using alcohothermal seeding method [20], namely consecutive spin-coating of ethanolic solution of zinc nitrate hydrate, $ZnNO_3{\cdot}6H_2O$ (Alfa Aesar) and thermal annealing (using a split-tube furnace system (Thermcraft, USA)) at 200°C in air for 1 h. The SZN was then grown by simply immersing the FTO/Al-loaded ZnO nanoseed substrate into a growth solution that contains an equimolar (0.3 M) aqueous solution of $ZnNO_3{\cdot}6H_2O$ and 0.03 M hexamethylene tetramine. The growth reaction was carried out under microwave irradiation (power ca. ∼1100 W) inside a microwave oven (Panasonic) for 20 s. The sample was then taken out, washed in a copious amount of pure water, and dried using a flow of nitrogen gas. The as-prepared SZNs were then annealed for 1 h in the air at 350°C to remove any organic residue on the sample and to obtain a better ZnO crystallinity. From this procedure, a high-density SZN structure on the FTO substrate (confirmed by X-ray diffraction (XRD) and field emission scanning electron microscopy (FESEM) results) was obtained. In this study, the SZN with five different porous densities were prepared by simply varying the Zn precursor ($ZnNO_3{\cdot}6H_2O$) concentrations in the reaction, namely 0.01, 0.02, 0.03, 0.04 and 0.05 M. Other reagents and procedures used in this work were kept unchanged.

The Ag nanoparticle (AgNPs)-loaded SZN (Ag-SZN) were prepared by firstly immersing the SZN-coated FTO substrate into a 20 ml aqueous solution that contains 0.5 ml of 0.01 M $AgNO_3$ (Sigma-Aldrich, USA) and 0.5 ml of 0.01 M trisodium citrate (WAKO Chemical, Japan). The sample was left for 30 min undisturbed to facilitate Ag^+ ions adsorption onto the SZN surface. After that, 0.1 ml of ice-cooled $NaBH_4$ (0.1 M) was injected into the solution. The colour of the solution changed from colourless to yellow, indicating the formation of Ag both in the solution and on the surface of SZN. The reaction was then left undisturbed for another 1.5 h at room temperature, to facilitate the effective growth of AgNPs on the surface of SZN. The sample was then taken out, washed with a copious amount of pure water, and dried with a flow of nitrogen gas. Finally, the sample was annealed in air at 200°C for 1 h to remove any organic residue on the sample surface.

2.2 *Characterizations*

The morphologies of the unloaded and Ag-SZN were obtained using a field emission scanning electron microscopy (FESEM) Zeiss Supra 55VP FESEM apparatus. The phase and structural properties of the unloaded and Ag-SZN were characterized by X-ray diffraction (XRD) measurements using Bruker D8Advance with CuKα radiation (λ = 1.541 Å) and scan rate as low as 2° min^{-1}. UV-Vis diffuse reflectance spectroscopy (Winlab, Hitachi, Japan) was used to obtain the optical properties of the sample.

3. Results and discussion

3.1 *AgNP-loaded SZN*

Standing ZnO nanosheet with controlled porous density on the FTO substrate surface has been successfully prepared using the present method. Figure 1 shows the typical surface

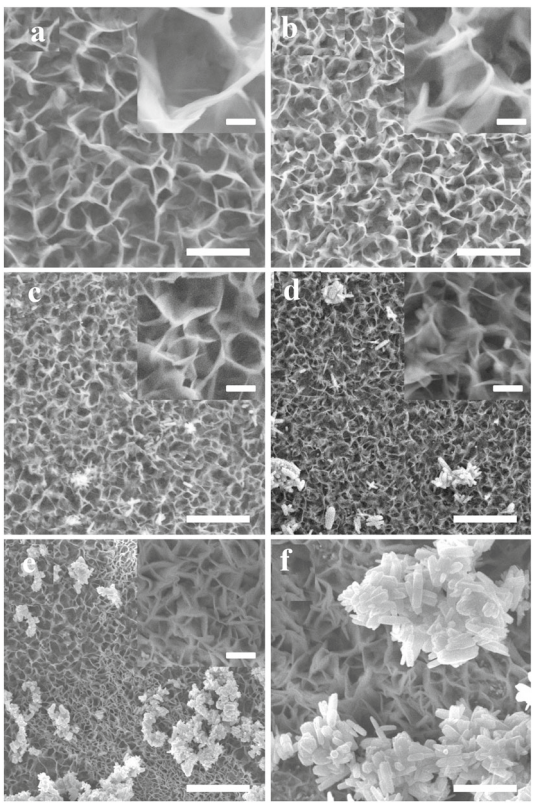

Figure 1. FESEM micrograph for SZNs morphology at various Zn^+ precursor molarities, namely (**a**) 0.01, (**b**) 0.02, (**c**) 0.03, (**d**) 0.04 and (**e**) 0.05 M. (**f**) A high magnification image for sample (**e**). Scale bars are 1 μm and 100 nm for insets and (**f**).

morphology of the SZN grown using five different Zn precursor concentrations, namely 0.01, 0.02, 0.03, 0.04 and 0.05 M. As shown in figure 1, the SZN is characterized by a continuously connected nanosheet structure that is vertically grown on the substrate surface, forming a porous surface structure. The thickness of the nanosheet is in the range of 10–15 nm and was found to have no significant dependency on the Zn precursors concentration used in the reaction. However, the pore size (the average edge-to-edge distance) decreases with the increase of ZnO precursor concentration in the reaction. For example, at low concentration (see figure 1a), the size of the pore is approximately 500 nm. The pore size effectively decreases when the precursor concentration was increased (figure 1a–e). At a relatively high concentration, i.e., 0.05 M (see figure 1e), the pore size is as low as ca. 50 nm. This produces SZN with high-pore density on the substrate surface, promising unique optical and electrical properties. A complete porosity data of nanosheet film grown from different ZnO precursor concentrations is summarized in table 1. The increase in the pore density upon the increasing of ZnO precursor concentration is simply related to the high-kinetic nature of the growth reaction at high precursor concentration, causing rapid growth and deposition of the ZnO nanostructure onto the surface [21,22]. Therefore, at this condition, the competitive nucleation characteristic of the reaction is high, resulting in the formation of smaller pore size, thus increases the density. Unfortunately, as can be seen from the figure, the use of high ZnO precursor concentration has caused unstability in the reaction that was indicated by an active formation of ZnO by-product in solution (ZnO nanorods), of which some of them are attached to the nanosheet surface. This could more or less distort the unique property of the porous nanosheet film. The results are shown in figure 1e and f (magnified images).

The formation of nanosheet structure has been understood as the effect of effective etching and passivation of (101) and (100) planes by the $Al(OH)_4^-$ complexes in the solution that is produced from the dissolution of the Al layer by hexamethylene tetramine [19]. This condition favours the growth of two-dimensional morphology instead of other morphologies, such as spherical or irregular shape nanostructures.

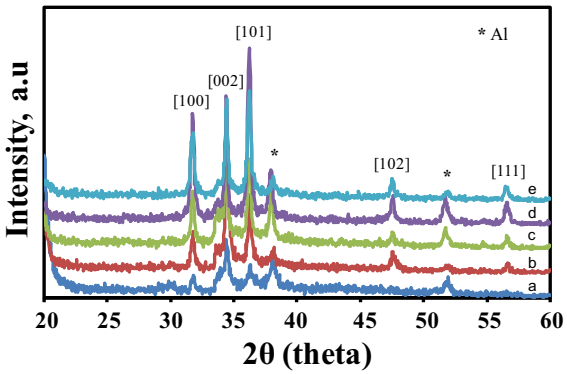

Figure 2. XRD spectra for SZNs morphology at various Zn^+ precursor molarities of (**a**) 0.01, (**b**) 0.02, (**c**) 0.03, (**d**) 0.04 and (**e**) 0.05 M.

Figure 2 shows the phase analysis result of the SZN that were prepared using five different Zn^+ precursor solutions, namely 0.01, 0.02, 0.03, 0.04 and 0.05 M. As can be seen from the figure, the entire sample shows a similar XRD pattern with the presence of five major peaks in the spectrum, namely at 2θ of 31.6, 34.3, 36.2, 47.5 and 56.6°. This XRD pattern agrees well with the standard XRD data (file no. 36-1451) for the pure ZnO phase with peaks at 2θ of 31.6, 34.3, 36.2, 47.5 and 56.6° corresponding to the XRD from the (100), (002), (101) (102), and (111) Bragg planes, respectively. It can be noted here that the SZN produce from the lower precursor concentration seems to be characterized by the (002) plane (*c*-axis plane) because of a high-diffraction intensity originated from this plane (see curve *a*). However, the XRD profile was effectively modified when the SZN was prepared using a higher ZnO precursor concentration (see curves *b* to *e*). At these concentrations, the SZNs were characterized by (101) plane with ratio diffraction intensity between (101) and (002) planes as high as 1.5, which is only 0.5 for sample *a*. It is also observed that the diffraction from the (100) plane is also high and comparable to the (002) plane with an intensity ratio between (100) and (002) in the range of 0.6 to 0.8, which is only 0.4 for the sample *a*. We assumed that the SZN wall should be characterized by the planes of (101) and (100). As the (101) and (100) planes for ZnO is a highly energetic surface, thus we expect peculiar optical and

Table 1. Average pore diameter for SZNs prepared at five different concentrations.

Zn precursor concentrations (M)	Average pore diameter (μm)	Optical band edge (eV)
0.01	1.683	3.310
0.02	1.350	3.305
0.03	0.941	3.290
0.04	0.729	3.290
0.05	0.654	3.290

electrical properties to be produced from this structure. In addition, from the spectra, the Al crystal peaks were also present, namely at 38.0° and 56.5°. This could be from the Al layer that is not completely consumed during the SZN formation. However, their intensity is relatively low and its effect on the optical and electrical properties of SZN is expected to be minimum.

We then grew AgNPs onto the surface of SZN by our previously reported technique that involves a simple immersion of the SZN sample into the solution of Ag colloidal reaction formation. After finishing the AgNP growth procedure for 1.5 h and followed by brief rinsing using pure water, we carried out a FESEM analysis to confirm the AgNPs formation on the SZN surface. The result is shown in figure 3. As shown in figure 3, the AgNPs have been effectively attached to the surface of the SZN. They are indicated as bright dotted particles as shown in the high-resolution FESEM image in the inset of the corresponding FESEM image (see figure 3a–e). Their size range from 15 to 20 nm. The elemental analysis using electron energy dispersion spectroscopy (EDS) might further verify the AgNPs existence on the surface of SZN. Nevertheless, due to the limited access to the technique, we cannot provide them at this stage. However, the presence of such bright nanoparticles on the surface of SZN after a treatment in the AgNPs colloidal reaction is a clear indication that the AgNPs successfully decorate the SZN. Notwithstanding, the XRD and optical absorption analyses (will be discussed in the following) have confirmed that the AgNPs are existing in SZN thin films.

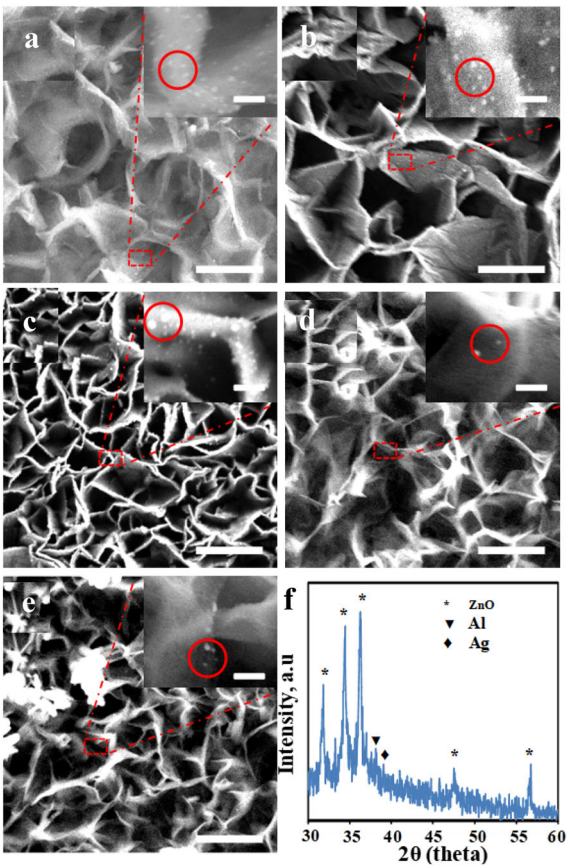

Figure 3. (**a**–**e**) FESEM image of vertical ZnO nanosheet from different precursor concentrations, as in figure 1, decorated with AgNPs. Panel (**f**) is the XRD pattern of the sample. Scale bars are 1 μm and 100 nm in the inset.

We then performed an XRD analysis of the sample to further verify the existence of the AgNPs in the sample. A sample with medium Zn precursor concentration, i.e., 0.03 M, was used in the analysis. As has been expected, the Ag crystalline phase is observed in the XRD spectrum along with the ZnO and Al (see figure 3f). The SZN decorated with AgNPs should produce special properties so that unusually high performance in the application would be obtained. As shown in figure, the peak intensity of the AgNPs is indeed weak if compared even with the Al. Because the XRD peak intensity is related to the crystallite size ratio of the component in the sample where SZN, particularly, majorly composes the sample, the diffraction peaks are dominated by the SZN leaving other crystallite components weakly observed in the XRD pattern. The Al peak intensity is higher than the AgNPs, which could be due to the same reason where Al layer crystallite size is bigger than AgNPs. It is because Al layer is not completely consumed during the catalytic projection of SZN. The Al layer was deposited on the entire surface of the substrate with a thickness of approximately 30 nm. An incomplete consumption of Al layer during the growth of SZN could leave the Al layer with crystallite size higher than AgNPs (size approximately 15 nm). Thus, the Al layer XRD peak is higher than AgNPs.

We carried out a UV-Vis absorption spectroscopy technique to further verify the presence of AgNPs on the surface of SZN and to evaluate the optical properties of the SZN under the influence of AgNPs attachment. Figure 4a shows their corresponding optical absorbance. It is seen that excitonic absorption of ZnO (at the wavelength of ca. 360 nm) [23] along with localized surface plasmon resonance absorption of Ag (ca. 419 nm) [24] are observed in the spectrum. This certainly is a further confirmation of the AgNP's existence on the surface of SZN. As can be seen from figure 4b and table 1, it can be estimated that there is a modification in the optical bandgap of the SZN when its dimension is altered due to the dimensional effect at this nanostructure regime or decorated with the AgNP. We then extrapolate the Tauc plot from the absorbance spectrum of the sample to see the impact of dimension modification and the AgNP attachment on the optical properties of the SZN (see figure 4b). For example, the thinnest SZN (curve 1 in figure 4b) decorated with the AgNPs has an optical band edge as high as 3.31 eV. It gradually decreases with the increase of thickness and has an optical energy gap as low as 3.29 eV in the thickest ZnO nanosheet (curve 5 in figure 4b). Because the AgNPs dimension and density on the SZN surface are more or less similar on each SZN

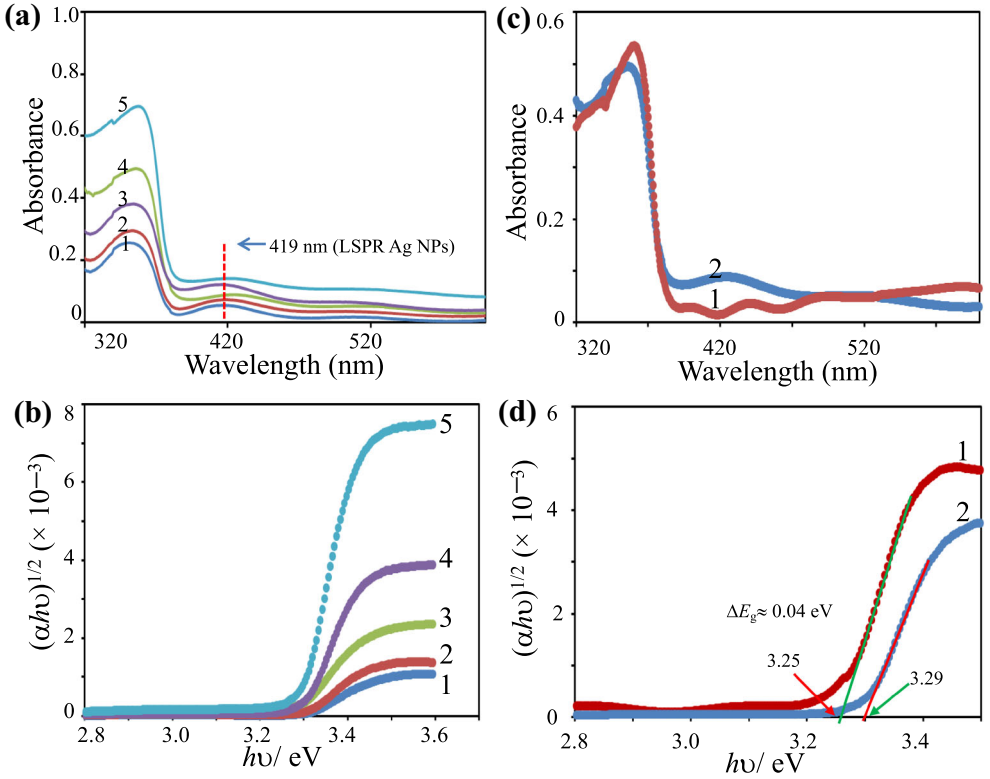

Figure 4. (**a**) Optical absorbance of the vertical ZnO nanosheet decorated with AgNPs with different ZnO precursor concentrations, i.e., 0.01 (1), 0.02 (2), 0.03 (3), 0.04 (4) and 0.05 M (5). (**b**) Corresponding Tauc plot of the samples. (**c**) Comparison of optical absorption properties of pristine ZnO nanosheet (curve 1) and AgNPs decorated ZnO nanosheet (curve 2), and (**d**) their corresponding Tauc plot showing modification on the optical bandgap.

sample, as expected, we can remark that the energy gap decrease should be due to the increase in SZN dimension and thickness [25]. To understand the extent effect of AgNP impact on the optical properties of the SZN, we compared the optical properties of pristine SZN with the ones decorated with AgNPs that were prepared using similar ZnO precursor concentration (0.04 M). The result is shown in figure 4c and d. We noticed that the band edge of the ZnO is blue-shifted up to 0.04 eV with the attachment of AgNPs (figure 4d). The pristine SZN optical band edge is approximately 3.25 eV. This result is quite surprising as surface attachment of the AgNPs in fact can induce the bulk optical properties of the SZN, which could be via many ways such as carrier equilibration effect, Fermi level alignment between the Ag and ZnO, etc. Normally, such transformation in the bulk optical properties of material should be produced by a strong perturbation from the external agent, in this case, the AgNPs [26]. However, considering the low thickness of the SZN, i.e., approximately 15 nm, bulk electronic modification in the SZN by the AgNPs attachment would be possible. This certainly is followed by modification of the overall physicochemistry properties of the SZN. Enhanced performance in the existing application is expected from the Ag-decorated SZN.

We again remark that the AgNPs have effectively modified the optical properties of SZN, which was achieved via a two-step process. We predict that, although the present result uses FTO as the substrate, the method should also be extended to grow SZN on other substrates, such as glass. While the two-step method could be a tricky and lengthy process, notwithstanding, it offers a sophisticated way to attain a preserved morphology of the SZN and the AgNPs. A simple, one-pot reaction process has been used to grow and modify the electrical and optical properties of the ZnO nanostructure as in the formation of Ag-ZnO nanorod [27]. Nevertheless, although it might produce effective modification on the optical properties of ZnO nanostructure, it may induce a deformation on the two-dimensional crystal growth in the ZnO. Therefore, a special effort could be conducted to realize a one-pot process for the preparation of AgNPs-decorated SZN.

Nevertheless, the Al system is still detected in the sample with significant content as shown in the XRD analysis result. This is the result of the Al layer that is not fully consumed during the catalytic growth of SZN. It may certainly generate a strong effect on the optical and electrical properties of the SZN. At this stage, the approach to remove or decrease the Al content in the SZN is not yet obtained.

We assumed that the use of appropriate thickness of Al layer or the use of an additional catalyst to accelerate the Al consumption might remove or reduce the Al presence in the SZN. This effort is being pursued and the result will be reported separately.

4. Conclusions

The method to prepare SZN on the substrate surface has been presented via the microwave-assisted hydrothermal method. The SZN has a length of up to 1 μm and thickness can be as low as 10 nm. We also discovered that the AgNPs of size up to 20 nm can induce change in the optical absorption properties of the SZN. In the typical process, the optical energy band edge of the SZN blue shifts as high as 0.04 eV upon being decorated with the AgNPs. This is unusual and is assumed due to the thin structure of the nanosheet so that the AgNPs attachment on the surface can strongly distort both the surface and the bulk lattice of the SZN. This system should find extensive application in sensors, photocatalysis and solar cells.

Acknowledgements

We thank the Ministry of Higher Education of Malaysia for supporting this project under FRGS/1/2019/STG02/UKM/02/3 grant.

References

[1] Polarz S 2011 *Adv. Funct. Mater.* **21** 3214
[2] Burda C, Chen X, Narayanan R and El-Sayed M A 2005 *Chem. Rev.* **105** 1025
[3] Mclaren A, Valdes-Solis T, Li G and Tsang S C 2009 *J. Am. Chem. Soc.* **131** 12540
[4] Alivisatos A P 1996 *Science* **271** 933
[5] Ali Umar A and Oyama M 2005 *Cryst. Growth Des.* **5** 599
[6] Ali Umar A and Oyama M 2006 *Cryst. Growth Des.* **6** 818
[7] Ali Umar A and Oyama M 2008 *Cryst. Growth Des.* **9** 1146
[8] Ali Umar A, Oyama M, Mat Salleh M and Yeop Majlis B 2010 *Cryst. Growth Des.* **10** 3694
[9] Viswanatha R, Sapra S, Satpati B, Satyam P, Dev B and Sarma D 2004 *J. Mater. Chem.* **14** 661
[10] Schoenhalz A L, Arantes J T, Fazzio A and Dalpian G M 2010 *J. Phys. Chem. C* **114** 18293
[11] Zhao J-H, Liu C-J and Lv Z-H 2016 *Optik* **127** 1421
[12] Quy C T, Hung C M, Van Duy N, Hoa N D, Jiao M and Nguyen H 2017 *J. Electron. Mater.* **46** 3406
[13] Mintcheva N, Aljulaih A A, Wunderlich W, Kulinich S A and Iwamori S 2018 *Materials* **11** 1127
[14] Tan S T, Ali Umar A, Balouch A, Yahaya M, Yap C C, Salleh M M *et al* 2014 *ACS Comb. Sci.* **16** 314
[15] Orou S F C, Hang K J, Thien M T, Ying Y L, Diem N D N, Goh B H *et al* 2018 *J. Ind. Eng. Chem.* **62** 333
[16] Al-Hinai M H, Sathe P, Al-Abri M Z, Dobretsov S, Al-Hinai A T and Dutta J 2017 *ACS Omega* **2** 3157
[17] Rahman M Y A, Umar A, Taslim R and Salleh M M 2013 *Electrochim. Acta* **88** 639
[18] Tan S T, Umar A A and Salleh M M 2016 *J. Phys. Chem. Solids* **93** 73
[19] Ridha N J, Umar A A, Alosfur F, Jumali M H H and Salleh M M 2013 *J. Nanosci. Nanotechnol.* **13** 2667
[20] Tan S T, Umar A A, Balouch A, Yahaya M, Yap C C, Salleh M M, Oyama M *et al* 2014 *Ultrason. Sonochem.* **21** 754
[21] Viswanatha R, Amenitsch H and Sarma D 2007 *J. Am. Chem. Soc.* **129** 4470
[22] Viswanatha R, Santra P K, Dasgupta C and Sarma D 2007 *Phys. Rev. Lett.* **98** 255501
[23] Laskowski R and Christensen N E 2006 *Phys. Rev. B* **73** 045201
[24] Nafisah S, Saad S, Umar A A, Plucinski K, Lis M, Maciaga A *et al* 2015 *Opt. Appl.* **45** 263
[25] Miao L, Tanemura S, Tanemura M, Lau S P and Tay B 2007 *J. Mater. Sci. Mater. Electron.* **18** 343
[26] Hewlett R M and McLachlan M A 2016 *Adv. Mater.* **28** 3893
[27] Sarkar S and Basak D 2013 *CrystEngComm.* **15** 7606